HELICOPTER MATHEMATICAL MODELS AND CONTROL LAW DEVELOPMENT
FOR HANDLING QUALITIES RESEARCH

Robert T. N. Chen, J. Victor Lebacqz, and Edwin W. Aiken
NASA Ames Research Center, Moffett Field, CA 94035

Mark B. Tischler
U.S. Army Aeroflightdynamics Directorate
NASA Ames Research Center, Moffett Field, CA 94035

SUMMARY

Progress made in joint NASA/Army research concerning rotorcraft flight-dynamics modeling, design methodologies for rotorcraft flight-control laws, and rotorcraft parameter identification is reviewed in this paper. Research into these interactive disciplines is needed to develop the analytical tools necessary to conduct flying qualities investigatins using both the ground-based and in-flight simulators, and to permit an efficient means of performing flight test evaluation of rotorcraft flying qualities for specification compliance. The need for the research is particularly acute for rotorcraft because of their mathematical complexity, high order dynamic characteristics, and demanding mission requirements. The research in rotorcraft flight-dynamics modeling is pursued along two general directions: generic nonlinear models and nonlinear models for specific rotorcraft. In addition, linear models are generated that extend their utilization from 1-g flight to high-g maneuvers and expand their frequency range of validity for the design analysis of high-gain flight control systems. A variety of method ranging from classical frequency-domain approaches to modern time-domain control methodology that are used in the design of rotorcraft flight control laws is reviewed. Also reviewed is a study conducted to investigate the design details associated with high-gain, digital flight control systems for combat rotorcraft. Parameter identification techniques, both frequency- and time-domain approaches, developed for rotorcraft applications are reviewed. The paper describes the results of both the in house research and other related efforts via contracts to industry, grants to universities, and international collaborative programs.

INTRODUCTION

This paper summarizes the results of the joint NASA/Army efforts in the development of the helicopter math models and the flight control laws for handling-qualities research using both the ground-based and in-flight simulators at Ames Research Center (ARC). The paper also discusses the development of state estimation and parameter identification techniques using flight test data. These techniques provide a capability to improve the fidelity of the math models and permit an

efficient means of conducting flight test evaluation of helicopter flying qualities for specification compliance.

Efforts began in 1975 to develop a generic flight-dynamics model suitable for real-time simulation motivated primarily by the need to conduct piloted ground-based simulation to determine the helicopter handling qualities requirements for the Army's new doctrine of nap-of-the-Earth (NOE) operations and for airworthiness standards for civil operations in the terminal area. Efforts were also directed at developing simpler math models expressly for use in the investigation of control and display laws to enhance the capability of military helicopters to perform NOE missions under night/adverse weather conditions or to conduct aerial combat. In addition, simulation models for the UH-1H VSTOLAND and the variable-stability CH-47B research helicopter were developed to support the in-flight research programs using the two aircraft.

Until 1981, these analytical flight-dynamics math models were developed mainly for use on the Ames ground simulators which at that time had only a moderate level of computational speed and capacity, typical of the Xerox Sigma class of digital computers. To stay within a reasonable computational cycle time, the frequency range of applicability of these simple models was somewhat limited. They included at most the flapping-dynamics and the main rotor rotational-speed degrees of freedom (DOF), in addition to the basic 6 DOF of the rigid-body dynamics. With the introduction of a CDC 7600 machine dedicated to the Vertical Motion Simulator (VMS) in 1982, the level of sophistication of the helicopter flight-dynamics models was expanded both in the calculation of the aerodynamic forces and moments and in the number of degrees of freedom in the model. Details in the simulation for the engine and its fuel control system were also expanded to be compatible with the level of sophistication of the simulation for the airframe and its flight control system. These high-frequency, full-flight-envelope real-time simulation models for the aircraft/engine systgem were validated with flight test data and were used to examine helicopter flight characteristics near the boundaries of the operational flight envelopes. They were also used as a basis for an investigation of potential benefits of integrating flight and propulsion controls.

To provide for design analyses of control and display laws, linear models were generated from the nonlinear simulation models. In particular, a new procedure was developed to permit linearization from a nonlinear model that simulates a coordinated or uncoordinated, steep, high-g turn. This new analytical procedure was used to systematically examine the rotorcraft coupling characteristics in high-g turns, the significance of the direction of turns for single-rotor helciopters, and the impact of high-g maneuvers on the performance of the stability-and-control-augmentation systems. In addition to extending the linear model from 1-g flight to high-g maneuvers, the frequency range of validity of the linear model was also expanded by including high-order effects such as rotor and inflow dynamics. These high-order models were used in the analytical and flight investigation of the influence of rotor and other high-order dynamics on helicopter flight-control-system bandwidth.

Several methods have been used to design helicopter flight control laws for handling-qualities investigations. Early on, classical frequency-domain methods were used in the design of control laws to provide a variety of control response characteristics for experimental determination of their suitability for various mission tasks. Time-domain, linear quadratic regulator theory was subsequently applied to the design of a high performance stability-and-control-augmentation system for a hingeless rotor helicopter to be used for piloted evaluation on a ground-based simulator. The linear quadratic regulator (LQR)-based, low-order compensation method developed at Stanford University was applied to the design of a hover hold system for the CH-47 research helicopter and was evaluated in flight on that aircraft. An optimal cooperative-control synthesis method developed originally for fixed-wing aircraft at Purdue University which includes an optimal pilot model in the design procedure, was extended and applied to a CH-47 helicopter and was evaluated in a piloted ground-based simulation. In collaboration with industry, advanced control laws were developed for the Advanced Digital/Optical Control System (ADOCS) demonstrator helicopter based on single-axis model-following control concepts. A multivariable model-following control system was developed for the variable-stability CH-47B to enhance its in-flight simulation capability. In addition, problems associated with the design and implementation of high-bandwidth digital control systems for combat rotorcraft were investigated in order to reduce the cost and time involved in control system modifications or redesigns often required during the flight test phase of a development program.

It is essential that the mathematical models for real time simulations or for analyses and syntheses of flight control laws be evaluated based on comparison with flight test data. To determine how well a simulation model represents the real rotorcraft, the trim characteristics and the response-time histories from flight tests must be compared with those predicted from the model. If the comparison between the test and the calculated data is clearly unacceptable, the correlation must be improved. This can be achieved through the use of parameter identification techniques. The development of parameter identification techniques suitable for rotorcraft application has also been an active area of research at ARC; these techniques have used both time- and frequency-domain approaches.

In the following sections, the results of both the in-house research and the related efforts via contracts to industry, grants to universities, and international collaborative programs are described.

REAL-TIME FLIGHT DYNAMICS MATHEMATICAL MODELS FOR ROTORCRAFT

The development of rotorcraft flight dynamics math models at ARC has been prompted primarily by the need for real-time, piloted ground-based simulation. The complexity of a rotorcraft math model for real-time, pilot-in-the-loop simulation depends on the purpose for which the model is to be used. The math model complexity may be conveniently classified using the two major factors: (1) levels of detail in representing the dynamics of the rotorcraft and (2) levels of sophistication in

calculating the rotorcraft forces and moments, especially for the rotor systems. The first factor determines the validity of the model in terms of the frequency range of applicability. For digital computation in a real-time simulation, the frequency range of interest sets the maximum permissible cycle time. The second factor determines the domain of validity in the flight envelope of the rotorcraft. These two factors together dictate the requirements for simulation computer hardware, software, and programming techniques.

Table 1 shows a list of rotorcraft math models for pilot-in-the-loop simulations. Depending on specific applications, these models reflect differing levels of completeness in representing the aerodynamics and rotor dynamics. The term linear aerodynamics implies simplications such as small angles of flapping and inflow, and use of simple strip theory with no consideration of compressibility or stall. Models with such simplifications can be used for exploratory investigations of handling qualities of a generic nature within limited regions of the flight envelope. However, for investigations involving exploration to the edges of the flight envelope, then even in generic studies the effects of compressibility, stall, and other nonlinearities must be included. Also, nonlinear effects must be included in the simulations whenever the characteristics of specific rotorcraft are investigated. The rotor dynamic modes include flap, lag, rpm, and inflow degrees of freedom. These rotor dynamic modes are generally of much higher frequency than those of the rigid-body modes. The most important rotor dynamic mode with regard of the interaction with the rigid-body modes is the flapping-regressing mode; therefore, it is generally included in flight dynamics simulation studies. However, for simulation investigations involving the use of high-gain feedback control, the inclusion of lag and other degrees of freedom may also be required.

The math model development has been pursued along the two general directions: generic models and models for specific rotorcraft.

Generic Models

Efforts began in 1975 to develop a simplified generic flight-dynamic model for exploratory pilot-in-the-loop simulation investigations on ground-based simulators that at that time had only moderate computational speed and capacity, typical of the Xerox Sigma class of digital computers. To stay within a reasonable computational cycle time (on the order of 40 ms), the frequency range of applicability of the model was necessarily limited. It included only the flapping dynamics and the main rotor rotational degrees of freedom, in addition to the basic 6 DOF of the rigid-body dynamics. The overall arrangement of the simulation model, which is called "ARMCOP" (refs. 1-3) is shown in figure 1. The model elements are: (1) main rotor, (2) tail rotor, (3) empennage, (4) fuselage, (5) engine-dynamics-and-rpm governor, and (6) control systems. The model elements denoted T_i in figure 1 are required to achieve transfer of velocities, forces, and moments from one axis sytem to another.

The main rotor model assumes rigid blades with rotor forces and moments radially integrated and summed about the azimuth, using essentially linear aerodynamics

as discussed earlier. The flapping equations of motion explicitly contain the primary design parameters, namely: flapping-hinge restraint, hinge offset, blade Lock number, and pitch-flap coupling. The tail rotor is assumed to be a teetering rotor without cyclic pitch and without including the tip-path plane dynamics. The empennage aerodynamics are modeled with a lift-curve slope between stall limits and a general curve fit for large angles of attack. The fuselage aerodynamic model uses a detailed representation over a nominal angle of attack and sideslip range of ±15°, and it uses a simplified curve fit at large angle of attack or sideslip. The helicopter model has a generalized control system, as shown in figure 2, which accepts inputs from the pilot, facilitates control augmentation and stability augmentation, and provides for mechanical control mixing or phasing of the cyclic inputs. In addition, a simplified engine/governor model, atmospheric turbulence, and a linearized six-degree-of-freedom dynamic model for stability and control analysis are included.

Some improvements have been made to this model to permit piloted simulator investigations of the engine-out operations (refs. 4, 5). The model has been expanded to include representation of some of the aerodynamic effects of low speed, low altitude, and steeply descending flight (refs. 6, 7). The effect of low-speed, low-altitude flight on main rotor downwash was obtained by assuming a uniform-plus-first-harmonic inflow model and then by using wind tunnel data in the form of hub loads to solve for the inflow coefficients. The results are given as a set of tables for the inflow coefficients as functions of ground proximity, angle of attack, and airspeed. For steep descending flight in the vortex-ring state, the aerodynamic effects were modeled by replacing the steady induced downwash derived from momentum theory with an experimentally derived value and by including a thrust-fluctuation effect caused by vortex shedding. The induced downwash and magnitude of the thrust fluctuations were represented as functions of angle of attack and airspeed.

This model has been used extensively in experimental design analyses and ground-simulator investigations of helicopter handling qualities for NOE operations (ref. 8), for helicopter air combat (refs. 9, 10), and for civil operations in the terminal area (refs. 11-13). The model has also been modified and/or configured to simulate other specific helicopters for handling qualities and flight control research within government agencies, in industry, and in the university. Continuing improvements of the model have been sought through grants in the areas of aerodynamic representation in ground proximity (refs. 14-16) for research in NOE mission tasks and of dynamics details to expand the frequency range of applicability of the model.

A simpler generic model (called "TMAN") was developed for use as the simulation model for the opponent (red) helicopter in the first helicopter-air-combat simulation at ARC (ref. 9). Because of computer capacity limits, the model was required to be relatively simple. Even so, it is capable of realistic maneuvers at hover, of low speeds, and in forward flight, and is easy to fly with a simple set of controllers. The model uses quasi-static linear stability and control drivatives for its aerodynamic representation, but it also uses the complete nonlinear kinematic and

gravitational terms. When configured for the simulation of the red helicopter, it had the following specific characteristics: an attitude command system for pitch and roll at hover and for low-speed flight; and an altitude-rate command and a yaw-rate command system in the vertical and directional axes, respectively. In forward flight, the pitch and roll axes were transformed into angular rate command systems while the directional axis provided an automatic-turn-coordination feature. The model is very easy to modify to achieve other desired stability-and-control response characteristics, and as such it was used extensively as both the blue and red helicopters in the subsequent helicopter air-combat simulations (ref. 17). In addition, it is currently being used in helicopter human-factors laboratory experiments and simulations.

Specific Rotorcraft Math Models

Several flight-dynamics models for specific rotorcraft have also been developed in-house or jointly with the manufacturers. Some of these were developed by modifying the generic ARMCOP model described earlier. Other models such as UH-1H, CH-47B, UH-60, AH-64A, and XV-15 were developed separately. These math models are briefly described below.

UH-60 ARMCOP- The ARMCOP model was modified to allow the simulation of the UH-60 Black Hawk helicopter (ref. 18). This model has been used for piloted simulator investigations of advanced flight control systems for Army helicopters (ref. 19) and a Navy-sponsored piloted simulation of shipboard landings using the SH-60 Sea Hawk (ref. 20). The modifications included the effects of a canted tail rotor, a variable-incidence horizontal stabilator, and the UH-60 pitch-bias actuator. In addition, the ARMCOP fuselage model was significantly modified to incorporate UH-60 fuselage aerodynamics, based upon extensive wind-tunnel test data, and a representation of the UH-60 engine and governor dynamics implemented using the generic model available in ARMCOP.

UH-1H/VSTOLAND and BO-105 S3 ARMCOP- As part of a joint research program of the U.S. Army and the German Aerospace Research Establishment (DFVLR), under the Helicopter Flight Controls Memorandum of Understanding (MOU), a multivariable model-following control system (MFCS) has been developed for use in flight research. In the process of developing the MFCS, the performance of the system was first evaluated on a ground-based simulator at Ames using two helicopter models which have large differences in flight dynamics and control characteristics as well as in control system actuators. One of these is the NASA/Army UH-1H V/STOLAND helicopter and the other the DFVLR BO-105 S3 helicopter. Figures 3 through 6 from reference 21 show the typical control systems and the actuating systems of the two helicopters. The generic ARMCOP model was configured to simulate the flight dynamic characteristics of these two aircraft and the specifics of their control and actuator systems. In addition, the generic simple-engine dynamic model resident in the ARMCOP (fig. 7a) was configured to simulate the BO-105's engine and governor dynamics (fig. 7b), since its rotor rpm dynamics and limits have a strong impact on the collective rate limit allowable for the BO-105 S3 helicopter (ref. 21).

A109 ARMCOP- Under the MOU between the U.S. Army and Italy, the ARMCOP model is being configured to simulate the flight dynamics of an Agusta A109 helicopter. Efforts have been made to correlate the A109 ARMCOP model with the flight test data from the A109K tests conducted during the spring of 1986 in Italy. Current efforts include the development of the A109 digital SCAS for inclusion in the A109 ARMCOP model and the preparation for a piloted simulation on the VMS at ARC.

AH-64A/OH-58D- A model of the AH-64 Apache helicopter (ref. 22) was developed as part of an investigation of its control system and display requirements (ref. 23). The model initially consisted of six degree-of-freedom equations of motion with a full set of nonlinear gravitational and inertial terms. The aerodynamic forces and moments are expressed as the reference values and first-order terms of a Taylor series expansion about a reference trajectory defined as a function of longitudinal airspeed. This particular model allowed a simulation valid for small perturbations from level flight conditions for an airspeed range of -40 to 160 knots. Aerodynamic force and moment data in the form of trim conditions as well as stability and control drivatives were supplied by the manufacturer. Subsequently, the same model was used as the basis for a piloted simulator investigation of certain characteristics of the AH-64 Back-Up Control System (ref. 24).

A similar technique was employed to generate a simulation model of the OH-58D helicopter for a simulator investigation of directional control problems and requirements (ref. 25). In this case, the required aerodynamic force and moment data were generated using an off-line ARMCOP representation of that aircraft based upon input data supplied by the Army and the manufacturer. The model was further modified to include rotor RPM degree-of-freedom and certain nonlinear yaw-damping and control-sensitivity effects which were modeled as functions of relative wind magnitude and direction.

UH-1H ("UNCLE") Model- A model of a Bell UH-1H helicopter was developed specifically for use in flight dynamics investigations and for simulation of terminal-area guidance and navigation tasks (ref. 26). It has been used in simulations for the development of software for the navigation and guidance programs associated with an avionics system known as V/STOLAND (ref. 27) and for a simulator investigation of the effects of failures of the stability augmentation system (ref. 28). The model uses a quasi-static, main-rotor forces and moments representation similar to that of the classical Bailey-Wheatley type, and uses simple expressions for the contributions of the tail rotor, fuselage, and empennage.

CH-47B Model- Similar to the UNCLE model, this model was developed for use in real-time piloted ground-based simulations to support the in-flight research programs using the variable-stability CH-47B research helicopter. This nonlinear simulation model developed by the Boeing Vertol company (ref. 29) has been adapted for use in the ARC simulation facility (ref. 30). It is implemented in the ARC Sigma IX computer where it is operated with a digital cycle time of about 30 msec. The model uses a total-force approach in six rigid-body DOF; steady-state tip-path plane solutions for rotor flapping dynamics form the basis for the simulation of the rotors in this model. The model also includes an option for simulation of externally suspended slung-load equations of motion. This model option, along with

detailed slung-load equations of motion developed in-house (ref. 31), will expedite research in areas related to sling-load operations. The CH-47B model has been used in conjunction with flight research conducted on the CH-47B research helicopter to develop a multivariable model-following control system (ref. 32) and to verify, in-flight, a control-system-design method using modern control theory (ref. 33). These research activities related to the control laws development are further discussed later in the paper.

UH-60 (GENHEL)- As part of a joint Army/NASA program for ground-based simulator validation, a blade-element simulation model for the UH-60 Black Hawk was acquired from Sikorsky Aircraft (ref. 34). Unlike all the other models discussed previously, which were developed expressly for use on ground simulators which had only a moderate level of computational speed and capability (such as the Xerox Sigma class of digital computers), the Black Hawk model was intended for implementation on a CDC 7600 computer, which is a much more powerful machine than a Sigma computer. The UH-60 GENHEL model acquired from Sikorsky includes six rigid-body DOF as well as the main rotor flapping, lagging, air mass, and hub-rotational-speed DOF. It is a blade element model, rather than a total force-and-moment model, and as such, it covers the full range of angles of attack, sideslip, and inflow, without using small-angle assumptions. From this model, the computer code was written to execute in real time on the CDC 7600 computer (dedicated to the VMS). In addition, fidelity of the model has been improved considerably by NASA (ref. 35), notably in the area of engine and drive train modeling. Figure 8 taken from ref. 35 shows a block diagram representation of the simulation elements and their interactions. This improved high-frequency, full flight-envelope, real-time simulation model has been used to conduct the Black Hawk accident simulation investigations on the VMS. It also serves as a basis to investigate potential benefits of integrating flight and propulsion controls (refs. 36, 70).

Other Rotorcraft Mathematical Models- Also available at ARC are several specific rotorcraft math models developed for real-time simulation in a variety of projects. They include a math model for SH-2F (ref. 37), one for SH-3G (ref. 38), one for RSRA (ref. 39), and a math model for the XV-15 (ref. 40). The XV-15 simulation model, in addition to extensive use during the development phase of the aircraft, has been utilized in the ground simulator investigation of VTOL instrument flight rules airworthiness criteria (ref. 41). The model, along with some other models described previously has also been used in the investigations of high-g flight dynamics and high-order dynamic effects to be discussed next.

SMALL PERTURBATION FLIGHT DYNAMICS

Traditionally, the standard equations of airplane motion for small-disturbances from steady, symmetrical, rectilinear 1-g flight as the reference flight condition (refs. 42, 43) have been the basis for stability and control analyses, handling-qualities specifications (refs. 44-47), and design analyses of the stability-and-control-augmentation system (SCAS) for rotorcraft. However, modern military

rotorcraft are now being designed with a view toward expanding their roles in tactical missions such as combat rescue, antitank, and air-to-air operations that require high-g maneuvers that make frequent excursions to the limits of their maneuvering flight envelopes. Therefore, a new analytical framework is needed to permit a systematic examination of the flight dynamics and control characteristics of the basic aircraft and its SCAS to ensure that the overall aircraft-SCAS system will perform satisfactorily, not only in operations near 1-g flight but also in high-g maneuvers.

A fundamental characteristic associated with a rotorcraft with increasing load factor in high-g maneuvers is an increase in control effectiveness and damping, particularly in the pitch and roll axes. The extent of the increase depends, to a large measure, on the main rotor hub design. For a teetering-rotor helicopter, the control in pitch and roll is almost entirely through tilting the thrust vector of the main rotor; therefore, the increase in control effectiveness in these two axes is directly proportional to the load factor. At the other extreme, for a hingeless rotor the increase is much less because the direct hub moment, which produces most of the control power, is independent of the thrust level of the rotor system. The increase in the control effectiveness with the load factor has an obvious effect on the selection of the SCAS. Further, interaxis cross-coupling, such as pitch, roll, and yaw, that results from collective inputs and pitch-roll coupling which results from aircraft angular rates, also changes with load factor. The ramifications of these variations in stability-and-control characteristics for the handling qualities and the design of SCAs needed to be considered.

In addition to this extension of the linear model to high-g maneuvers, the frequency range of validity of the linear model must also be expanded for the design analysis of high-gain FCSs for rotorcraft to meet the requirements for demanding mission tasks such as NOE flight and aerial combat. In the design analysis of such high-gain control systems, it is now essential that high-order dynamics of the system components be adequately modeled, in contrast to past practice in which only the lower-frequency, quasi-static, rigid-body flight dynamics were used in the design of low-gain FCSs. Recent flight investigations that used a variable-stability CH-47B research helicopter at ARC showed that not only high-order elements such as rotor dynamics are required (refs. 48, 49, 32), but also other high-order effects such as dynamics of sensor filters, servo actuators, and data processing delays of the airborne computer must also be adequately modeled.

Inclusion of the air-mass dynamics associated with a lifting rotor has also been shown in recent studies (refs. 49, 51) to be important in the design of high-gain FCSs. The frequencies of the inflow dynamic modes are the same order of magnitude as those of the rotor blade flapping and lead-lag modes; therefore, the dynamic inflow has a significant influence on the aeromechanic stability of the rotor system. In the following sections, we will first discuss the linearization of the rotorcraft motion about a curved flightpath as a reference flight conditions, followed by a discussion of the high-order dynamics.

Linearization of Rotorcraft Motion About Steady High-g Turns

Small-perturbation equations of motion about a generic curved flightpath will result in a set of linear time-varying differential equations which generally is difficult to operate and to interpret. However, if the reference flightpath is chosen to be a steady turn, then the resultant small-perturbation equations of motion will be a set of linear time-invariant differential equations, similar to those obtained from steady rectilinear 1-g flight as the reference flight condition most commonly employed (e.g., refs. 42, 43). Before perturbation operations are applied, the steady reference flight conditions must be established first.

Algorithms have been developed (refs. 52-54) that permit efficient computations of 1) aircraft states and control positions in coordinated steady, steep turns and 2) the associated small-perturbation equations of motion. In developing these algorithms, special attention was given to the influence of sideslip which normally exists in asymmetrical rotorcraft in coordinated turns as discussed previously. Using these algorithms, a study was conducted to investigate the static and dynamic characteristics of several rotorcraft in coordinated, steep, high-g turns (ref. 55). The results indicate 1) that strong coupling in longitudinal and lateral-directional motions exists for rotorcraft in coordinated, high-g turns, 2) that for single-rotor helicopters, the direction of turn has a significant influence on flight dynamics, and 3) that an SCAS that is designed on the basis of standard small-disturbance equations of motion from steady, straight, and level flight and that otherwise performs satisfactorily in operations near 1 g becomes significantly degraded in steep, turning flight.

For some operations, such as in aerial combat, turns may intentionally be flown uncoordinated to reduce the turn radius. To investigate the extent to which the static and dynamic characteristics of asymmetric and symmetric rotorcraft in steep turns are influenced by the levels and direction of uncoordination, the algorithm developed expressly for coordinated turns was extended (ref. 56) to permit an efficient computation of the trim states and control positions in a general, uncoordinated turning maneuver. Table 2 gives the set of trim algorithms for general uncoordinated flight including both uncoordinated steep turns and uncoordinated rectilinear flight. The level and direction of uncoordination are represented by the magnitude and sign of the lateral accelerometer signal n_y (side force) at the aircraft center of gravity. The closed-form kinematic relationships shown in the table decouple the governing equations for a general, steady, uncoordinated turn and thereby greatly simplify the trim computation (to the extent comparable to the normal 1-g flight).

Once the steady, reference flight conditiolns are determined, the small-perturbation equations of motion are obtained in two steps: 1) by applying the perturbation operation on the Euler equations and on the kinematic equations that relate the time rate of change of pitch- and roll-attitudes to the angular rates about the body-axis system, and 2) by then imposing the constraints that the perturbations are from a steady turn. This development accounts for complete kinematic, inertial, and aerodynamic coupling. Also, the aerodynamic terms include a complete set of acceleration derivatives. Table 3 shows a simpler form of the stability and

control matrices in which the acceleration derivatives are neglected. The equations are given with respect to the general body-axis system and they are cast in the first-order, vector matrix format to which many efficient software packages can be readily adapted.

These equations were implemented in conjunction with the trim algorithms for generic uncoordinated, steep high-g turns in a variety of nonlinear simulation models (refs. 1, 34, 40) to investigate a tilt-rotor aircraft and two single-rotor helicopters in various levels of uncoordinated, high-g turning maneuvers at low speeds. The results show 1) that the aircraft trim attitudes in uncoordinated, high-g turns can be grossly altered from those for coordinated turns; and 2) that within the moderate range of uncoordinated flight (side-force n_y up to ±0.1 g), the dynamic stability of the rotorcraft is relatively insensitive. However, the coupling between the longitudinal- and lateral-directional motions is strong, and it becomes somewhat stronger as the sideslip increases (ref. 57).

The results of a recent study conducted in a European laboratory (ref. 58) generally confirmed those of ARC. In particular, their results also indicate that in high-g turns, the coupling between the longitudinal and lateral-directional motions is strong. Consequently, the conventional short-period approximation and other approximations (ref. 59) suitable for rectilinear cruise flight become inadequate for predicting stability and response characteristics of the helicopter in high-g turns. As in the Ames studies (refs. 55, 57), their results for turns also show that all the helicopter stability and control derivatives change with load factor (or bank angle). The variations in these derivatives are caused by aerodynamic, inertial, kinematic, and gravitational terms, but it is primarily the increased aerodynamic terms that have the most influence on the short-term dynamic modes.

Considerations for High-Order Dynamics

The increasing use of highly augmented digital FCSs in modern military helicopters has prompted a recent examination at Ames of the influence of rotor dynamics and other high-order dynamics on control-system performance. In the past, industry has predicted stability augmentation gains that could not be achieved in flight (ref. 60, fig. 9). The operators of variable-stability research helicopters have also been aware of severe limitations in feedback gain settings when attempting to increase the bandwidth of FCSs needed to assure good fidelity during in-flight simulations. Now, with an increasing emphasis on high-bandwidth mission tasks, such as NOE flight and aerial combat for military helicopters, coupled with the development of new rotor systems and the trend toward using superaugmented, high-gain, digital FCSs (refs. 19, 61, 62), there is a widespread need for improved understanding of these limitations.

Therefore, a study was conducted at ARC to correlate theoretical predictions of feedback gain limits in the roll axis with experimental test data obtained from the variable-stability CH-47B research helicopter. The feedback gains, the break frequency of the presampling sensor filter, and the computational frame time of the

flight computer were systematically varied. The results, which showed excellent theoretical and experimental correlation (fig. 10), indicate that the rotor flapping dynamics, sensor filter, and digital-data processing delays can severely limit the usable values of the roll-rate and roll-attitude feedback gains.

In addition to rotor flapping dynamics, inflow dynamics can be also significant in the design of high-gain FCSs for rotorcraft. Recent research (refs. 63-67) on dynamic inflow has shown that the frequencies of the inflow dynamic modes are of the same order of magnitude as those of the rotor blade flapping and lead-lag modes; therefore, dynamic inflow can produce significant changes in the modes of rotorcraft motion. A study was therefore conducted at Ames to investigate the effects of dynamic inflow on rotor-blade flapping and vertical motion of the helicopter in hover. Linearized versions of two dynamic inflow models, one developed by Carpenter and Fridovich (ref. 68) and the other by Pitt and Peters (ref. 67), were incorporated in simplified rotor-body models and were compared for variations in thrust coefficient and the blade Lock number (ref. 49). In addition, a good correlation was obtained between the results of linear analysis, and the transient and frequency responses measured in-flight on the CH-47B variable-stability helicopter. The linear analysis also shows that dynamic inflow plays a key role in destabilizing the flapping mode. the destabilized flapping mode, along with the inflow mode introduced by the dynamic inflow, results in a large initial overshoot in the vertical acceleration response to an abrupt input in the collective pitch. This overshoot becomes more pronounced as either the thrust coefficient or the blade Lock number is reduced.

The influence of the lead-lag degrees of freedom on the automatic-control-system design for a helicopter has recently been investigated analytically by Curtiss (ref. 69) under a NASA-ARC grant for near hover flight. He showed that attitude feedback gain is limited primarily by body-flap coupling, but the rate feedback gain is limited by the lag degrees of freedom. An experimental verification is needed.

Beyond the high-order effects caused by rotor and inflow dynamics, the propulsion system dynamics can also have a profound effect on the helicopter flight dynamics and handling qualities. The helicopter rotor and drive train systems have lightly damped torsional dynamic modes which are within the bandwidth of the engine fuel-control system. Traditionally, engine manufacturers use a sophisticated engine dynamic model in conjunction with a rather rudimentary model for the helicopter rotor/airframe dynamics when designing the control system. Helicopter flight dynamicists have used the opposite approach. As a result, the dynamic interface problems that are not anticipated in the design stage can surface later in the ground- or flight-test phases of a helicopter development program, requiring costly add-on modifications to rectify the problems. Therefore, it is important to model the propulsion system dynamics at the levels of sophistication compatible with those of the airframe dynamics in the design of both the fuel control system and the FCS (see ref. 70).

FLIGHT CONTROL LAWS DEVELOPMENT

A variety of methods have been used to design rotorcraft flight control laws for handling qualities investigations. They range from classical frequency-domain design methods to modern time-domain control methodology. Classical frequency-domain methods were first used in the design of control laws to provide a wide spectrum of control response characteristics for experimental determination of their suitability for various mission tasks. These designs were performed mostly in the continuous (or analog) s-domain. To expose potential problems associated with digital implementation, especially for high bandwidth digital control systems, an extensive case study based on the ADOCS was conducted in a discrete z-domain and w-domain.

Modern methods for time-domain control law design were subsequently employed in several case studies. Lienar quadratic regulator theory was applied to the design of a high-performance SCAS for a hingeless rotor helicopter for piloted evaluation on a ground-based simulator. An LQR-based, low-order compensator method was applied to the design of a hover hold system for the CH-47 research helicopter as part of the collaborative efforts with Stanford University. An optimal cooperative control-law-synthesis method, which includes an optimal pilot model in the design procedure, was modified and applied to a tandem-rotor helicopter and was evaluated in a piloted ground-based simulation. A multivariable MFCS was developed for the variable-stability CH-47B research helicopter to enhance its in-flight simulation capability.

Generic Control Laws for Various Types of Response Characteristics

Generic FCSs which can be configured to provide a variety of helicopter response characteristics including rate and attitude were implemented in the basic ARMCOP model (ref. 1) and the ARMCOP/UH-60 model (ref. 18) for handling qualities research. The general form of the SCAS that was incorporated in the ARMCOP model employs a complete state feedback as well as a control mixing structure that facilitates implementation of control crossfeed, with control quickening from each of the four cockpit control inputs. Also, the augmentation-system gains may be programmed as functions of flight parameters, such as airspeed (fig. 2). This constant-gain configuration was subsequently modified (ref. 20) to include dynamic compensation elements in order to represent the SH-60B for the handlibng qualities investigation of its shipboard operations.

A more complicated implementation of the generic FCS was incorporated in the ARMCOP/UH-60 for the development of the Army's ADOCS. As part of the ADOCS program, control laws suitable for an attack helicopter mission were synthesized, evaluated in piloted simulations of both visual (ref. 71) and instrument flights (ref. 72) under various meteorological conditions, and implemented in a UH-60 demonstrator helicopter. Figure 11 presents a block diagram of the FCS design for the ADOCS program. The primary flight control system (PFCS) shown in the figure was designed to yield satisfactory unaugmented flight by providing feed-forward command

augmentation and shaping. The advanced flight control system (AFCS) included both stabilization feedback loops and a feed-forward control-response model. Stabilization feedback loops were designed solely for maximum gust and upset rejection; no compromise for control response was necessary. The use of a control-response model allowed the shaping of the short- and long-term response to the pilot's control inputs independent of the stabilization level. Various control response and stabilization schemes were developed using this approach to control system design and were evaluated for the attack helicopter mission in conjunction with a range of integrated side-stick controller configurations. These generic configurations are identified in figure 12 in a matrix format.

A generic SCAS configuration was also incorporated in the XV-15 model to provide SCAS features such as rate command, attitude command, rate command/attitude hold, and the translational rate command, to be used for a ground simulation investigation of control actuator authority requirements (ref. 73) and of instrument-flight-rules airworthiness criteria for the tilt-rotor class of Vertical Takeoff and Landing (VTOL) aircraft (ref. 41). The mechanizations were kept as simple as possible so that the results could be easily understood. Consequently, the feed-forward and feedback loops in the generic SCAS configurations employ primarily constant gains with little dynamic shaping required.

Implementation Considerations for High-Gain Digital Control Systems

Proposed concepts for the Light Family Helicopter (LHX) and Joint Services Operational Tilt-Rotor Aircraft (JVX) are embodied in a complex, highly maneuverable, versatile vehicle with avionics systems which are as important to mission success as the airframe itself. Single-pilot and NOE operations require handling qualities which minimize the involvement of the pilot in basic stabilization tasks. These requirements will demand a full-authority, high-gain, multimode DFCS. The gap between these requirements and current low-authority, low-bandwidth rotorcraft flight control technology is considerable. Ongoing research aims at smoothing the transition between current technology and advanced concept requirements.

A study was conducted (ref. 74) to

1. extensively review the state-of-the-art of high-bandwidth digital control systems,

2. expose areas of specific concern for FCSs of modern combat rotorcraft, and

3. illustrate the important concepts in design and analysis of high-gain, digital systems with a detailed case study involving a current rotorcraft system.

A comprehensive case study based on the ADOCS Black Hawk was conducted. Methods for analyzing and designing high-bandwidth digital control systems were discussed and illustrated. Figure 13 (from ref. 74) diagrams a typical attitude control system, including the many elements needed for a practical digital system

implementation. The response of the actuator rate ($\dot{\delta}_{A_\theta}$) to a step command input at δ_{c_θ} is shown in figure 14 (30 Hz system). The solid curve is the result obtained using approximate (continuous system) methods. The digital-system exact response is shown as open and closed dots, the latter being the response at the even sampling instants. This figure shows that the even-sample instants are a very poor reflection of the complete digital system response. The approximate analysis gives a fairly good estimate fo the intersample behavior, although the level of "roughness" is underestimated.

Modern Control Methodology

Certain modern multivariable design methods have been applied to helicopter flight control. These methods include (1) a linear quadratic method, (2) a method that produces robust, low order compensators, (3) a multivariable model-following control technique, and (4) a quadratic optimal control synthesis method. These techniques are generally better than the classical methods in reducing the number of design iterations, especially for multivariable control problems such as helicopter flight control. All four design applications have been carried through piloted evaluations on ground-based simulators, and two have been carried all the way to in-flight evaluation on the variable-stability CH-47 research helicopter. Each of the four case studies is discussed briefly in the following.

Linear Quadratic Regular-Least Squares Design Method- This method consists of a two-stage design process: LQR theory is applied to determine appropriate feedback gains for the stability augmentation system (SAS), followed by the design of the control augmentation system (CAS) using a least-squares design method (ref. 75). This method was employed to design a stability-and-control-augmentation system for a hingeless rotor helicopter to meet a set of 10 performance criteria (ref. 76) derived from handling quality requirements. For the SAS design using the LQR methodology, constant weighting factors were used for state and control variables. The ratio of these factors was employed as a parameter in the selection of feedback gains to satisfy three of the 10 performance criteria for full and partial state feedback systems. For the design of the CAS, which consists of a matrix of cross-feed gains, a least-squares method was used to satisfy the remaining seven performance criteria. The design was performed at three flight conditions (hover, 70, and 130 knots) using a 6-DOF linear model that represents the hingeless rotor helicopter. The designed SCAS was then evaluated using nine degree-of-freedom equations, which include flapping motion, to determine the influence of rotor dynamics. The results indicate that the flapping/regressing mode does couple with fuselage motions and produces roll/regressing and pitch/regressing oscillatory modes (fig. 15) at frequencies below 2 Hz. These oscillatory modes are not present in rigid body equations; therefore, the SCAS gains determined by analysis of rigid body equations of motion should be evaluated using a model which includes at least the blade-flapping motion.

A piloted ground-based simulation was conducted on the Ames Flight Simulator for Advanced Aircraft (FSAA), which is a 6-DOF moving-base simulator, to evaluate

the merit of the designed SCAS. The experiment was performed using a combined longitudinal and lateral-directional task--flying a course of barriers combined with trees placed down the centerline of the barriers (ref. 50). The results of the experiment indicated that satisfactory handling qualities (level I) were achieved with the designed SCAS operational, in contrast to marginally acceptable handling qualities (near the borderline of level II and level III) that were obtained for the basic aircraft.

Robust, Low-Order Compensator Design Method- An LQG-based control design methodology was developed at Stanford University which produces robust, low-order control laws for multiinput, multioutput dynamic systems (ref. 33). The design method is illustrated by a flow diagram in figure 16. After proper model scaling to facilitate the choice of weighting matrices in the standard LQG method, an initial, stable full-order dynamic compensator (regulator/Kalman-filter pair) is obtained which provides the desired control characteristics. The order of the initial compensator is then reduced using two measures of mode sharing of the compensator as criteria for deciding which modes of the compensator can be eliminated. These two measures are the singular value of the residue matrix associated with that mode and the singular value weighted by the real part of the mode. The order reduction is then followed by reoptimization and implementation of a robust design for the simplified compensator. This step uses a gradient-search algorithm based on a finite-time quadratic performance index (ref. 77), which produces a design that is stable and has adequate performance at specified normal and off-normal operating conditions. The final design step involves the design of the feed-forward gains to generate the command outputs. A command output matrix is calculated from the steady-state controls for the desired outputs, in a manner similar to the least squares approach discussed in the preceding method (LQG-LS). These command outputs are then summed with outputs produced from the compensator.

The methodology was applied to the design of a velocity-command system and a hover-hold system for a tandem rotor helicopter. These two control systems were implemented on the variable-stability CH-47B research helicopter and were flight-tested during 1984. The results of the flight tests and a detailed description of the design methodology are presented in reference 33.

Multivariable Model-Following Control System- An explicit MFCS consists of three basic elements: (1) the "model," (2) the "plant" (the rotorcraft), and (3) the model-following control law as shown schematically in figure 17. The purpose of the control law is to ensure that the rotorcraft follows the model, whose equations of motion represent the desired or ideal dynamic characteristics for rotorcraft. An MFCS is an attractive scheme for achieving variable-stability characteristics for in-flight simulation because, in principle, model characteristics can be varied over wide ranges without requiring corresponding changes in the model-following control law. This method is particularly useful in a situation in which a model that is used in a ground-based simulation investigation can be duplicated for use in an airborne simulator to provide a direct comparison of the two studies. In addition to in-flight simulation, a wider application of the model-following concept may lie in the design of advanced augmentation systems for future generations of

rotorcraft. By incorporating the desired characteristics in the model, satisfactory handling qualities may be assured for the augmented rotorcraft. An example of using the concept is the automatic FCS of the ADOCS discussed in the preceding section where a set of single-input, single-output MFCSs is utilized.

The development of the multivariable model-following control system began on the ground simulator as part of a joint research program of the U.S. Army and the German Aerospace Research Establishment (DFVLR). The results of the ground-based investigations (refs. 21, 78) indicate that the performance of the MFCS is dependent on the dynamics of the explicit model and on the limitations of the actuating system. Increases in the model bandwidth placed higher demands on the control system and resulted in degraded model-following performance. Significant improvements in model-following performance were achieved when a control-law switching feature, which was designed to account for position- or rate-limited actuators, was included in the control system.

When the model-following control laws that were initially developed on the ground-based simulator were implemented and evaluated on the variable-stability CH-47 research helicopter (fig. 18), it became clear that improvements to the initial design were needed to compensate for large time delays caused by the high-order effects such as rotor dynamics, sensor filter dynamics, and computational time delays (ref. 48) as discussed in the preceding section. An analysis that used a high-order dynamic model exposed the basic limitations of the original design and resulted in the development of a final four-axes multivariable MFCS (fig. 19, ref. 32). The final system, which features a feed-forward control and a "pseudo-complementary" feedback-compensation scheme, achieves high-bandwidth control and excellent model-following performance. Figure 20 shows an example of the model-following performance in the roll axis. The model characteristics that were implemented were second-order attitude-command systems with natural frequencies of 1.4 rad/sec and damping ratios of 0.707. Details of the design, implementation, and flight-test development of the system are reported in reference 32.

Quadratic Optimal Cooperative-Control Synthesis- Similar to the LQR-LS design method discussed pregviously, the quadratic optimal cooperative control synthesis (CCS) method also uses LQR theory. However, the CCS method offers two distinct features. (1) The CCS method uses output feedback rather than full state feedback as the case of LQR-LS method, thereby making it simpler for implementation. (2) In contrast to the three preceding design methods, the CCS method requires, in principle, no detailed a priori design criteria, because an assumed analytic pilot-model structure is an inherent feature of the approach (fig. 21). This can be a great advantage in cases where no existing design criteria exist because of either the nature of aircraft being controlled or of the task being performed. The need for explicit a priori design criteria is eliminated through the use of an explicit optimal pilot model (depicted schematically in fig. 22); the pilot model is based only on the task to be performed. The SCAS is then designed to minimize the "workload" of the assumed pilot model while limiting the SCAS control inputs.

The CCS method was developed for and previously applied to the longitudinal SCAS design for a fixed-wing aircraft and was found, on a fixed-based ground

simulation evaluation, to compare favorably with the augmentation system currently being used on that aircraft. This design method was modified for application to the helicopter, which has more complex flight dynamics. Two CCS designs were obtained (using the original and modified methods) for a CH-47 helicopter and compared with two other designs based on classical frequency-domain method and LQR theory. Results from a fixed-base piloted simulation indicate that the modified CCS design compares favorably with the classical frequency-domain design (which was obtained using detailed a priori design criteria), and was superior to LQR design (ref. 79).

PARAMETER IDENTIFICATION

Parameter identification is a process of determining the coefficients or parameters in the set of equations of motion of the aircraft, called the model, by disturbing the aircraft with known test inputs. The general form of the model is assumed a priori or is derived from knowledge of the aircraft. Thus, parameter identification is a subfield of system identification, which is concerned with the more difficult problem of determining the model itself without assuming the form of the model. Parameter identification methodology may therefore be used to improve rotorcraft simulation models, to assess their handling-qualities characteristics, and to help develop better models for FCS design.

While significant progress has been made in the last two decades in the field of parameter identification for fixed-wing aircraft (refs. 80-82), progress has been relatively slow in its rotary-wing counterpart. Several important issues in rotorcraft parameter identification need to be resolved.

Unlike the flight dynamics of fixed-wing aircraft, the dynamics of rotary-wing aircraft are characteristically those of a high-order system, as discussed earlier. Significant interaxis coupling exists for single main-rotor helicopters; dynamic interactions exist between the engine and drive train/rotor system; and high-order effects such as rotor dynamics and inflow dynamics exist inherently in the system. The large number of degrees of freedom associated with the coupled high-order dynamics leads to a large number of unknown parameters that have to be identified, making it extremely difficult to achieve a successful application of system or parameter-identification techniques. Vibration levels of rotorcraft are high, a fact which causes high noise contamination in response measurements and makes it even more difficult to achieve accurate state estimation and parameter identification. Further, the basic rotorcraft are generally unstable, so only short flight records can be used for direct identification of the basic aircraft parameters or indirect identification of them with SCASs operational. Either case can cause difficulty for parameter identification: for the short-flight record, the information contents are likely to be inadequate for all the dynamic modes, and with SCAS operational, inputs can be highly correlated with output responses, if the design of test inputs is ignored.

Early efforts were made by the Army and NASA in the development of advanced time-domain techniques for rotorcraft state estimation and parameter identification (refs. 83, 84), in attempts to overcome some of the difficulties described previously. Considerable efforts were subsequently devoted to the development of frequency-domain techniques (refs. 85-87), thereby providing a better perspective from which to assess the two approaches, and leading toward the development of a unified time- and frequency-domain parameter identification methodology for rotorcraft in the future.

Time-Domain Parameter Identification

First applications of time-domain (digital) parameter identification techniques to rotorcraft by NASA and the Army at Langley and elsewhere employed a measurement error method--Newton Raphson (ref. 88) and a simpler advanced method using the Extended Kalman Filter algorithm (refs. 89, 90). Typical procedures of using these two parameter identification methods are shown schematically in figure 23 (ref. 91). Both methods include the initial step of using a digital filter to process the raw flight data to reduce the data noise content. Applications have been made to the identification of quasi-static, rigid-body stability-and-control derivatives of single-rotor helicopters and a tandem-rotor helicopter. Both methods give a gross underestimation of primary derivatives such as roll, pitch, and yaw damping; it is not uncommon for positive values of the damping derivatives to be identified using the quasi-static rigid-body model. If the lower-order model is used, large fitting errors in some response variables (e.g., vertical acceleration) are also apparent (fig. 24). The then-available identification software and the lack of measurements of the rotor blade motion have limited those applications to the identification of only the rigid-body quasi-static stability-and-control derivatives without considering the effects of rotor dynamics and other high-order effects discussed in the earlier sections.

In addition to adequate modeling of the vehicle/rotor system, two other areas must be addressed to accurately identify the stability-and-control parameters: (1) instrumentation and measurement data analysis and (2) test input design. A joint Army/NASA program involving both Ames and Langley was therefore initiated in 1976 with the aim of developing a comprehensive advanced technique for rotorcraft state estimation and parameter identification, which addressed all aspects of problems peculiar to rotorcraft. The techniques developed by a contractor (ref. 84) are illustrated in figure 25. Applications of some of these techniques have been made to the Rotor System Research Aircraft (refs. 92, 93) and to the Puma helicopter (ref. 94) under a NASA/UK (Royal Aircraft Establish) collaboration.

As part of an ongoing US/German MOU on helicopter flight control, an extensive joint study is being conducted to analyze the XV-15 database using both time domain and frequency domain techniques. The objectives of this study are to gain a better appreciation for the relative strengths and weaknesses of those two different approaches and to develop improved methods of identification for rotorcraft. The time domain approach used by the DFVLR of the Federal Republic of Germany (FRG)

(refs. 95, 96) is shown in figure 26. The data compatibility analysis and data analysis blocks shown in the figure are similar to the state estimation and parameter identification described in figure 25, although different in detailed computational algorithms. The frequency domain approach employed by the U.S. Army in conjunction with this MOU effort is discussed next.

Frequency-Domain Parameter Identification

The frequency-domain-identification approach developed at ARC (refs. 85, 86) is shown in figure 27. Flight data are generated using frequency-sweep inputs for model extraction and step inputs for model verification. Two typical, concatenated, lateral-stick frequency sweeps completed during the hover flight tests of the XV-15 are shown in figure 28(a) with the corresponding roll rate response shown in figure 28(c). Pilot-generated, rather than computer-generated, inputs are used. The frequency-sweep input is especially well suited to the frequency-domain identification procedure because: (1) the wave form is roughly symmetric about the trim condition so that the aircraft motions are not excessive and the aircraft dynamics are likely to stay within the linear range; (2) the input and output wave forms are smooth and regular, so the resulting spectral functions are well behaved; and (3) the input autospectrum is generally constant over the desired frequency range.

For the spectral analysis, the ARC approach employs methods based on the Chirp z-transform to extract high-resolution frequency responses between selected input and output pairs. The identification results are presented in Bode-plot format: magnitude and phase of the output to the input vs. frequency (fig. 27). These results are nonparametric since no model structure has been assumed. As such, they can be used directly for FCS design or handling-qualities-compliance testing. These nonparametric identification results can also be compared directly with those obtained from real-time and nonreal-time simulations to expose limitations and discrepancies in the simulator models. Approximate transfer functions and modal characteristics may also be obtained by fitting the identified frequency-response plots with assumed analytical models of transfer function. The results are parametric models that are useful for transfer-function-based control-system-design studies and for handling qualities specifications given in lower-order equivalent-system terms. Since this fitting procedure is completed after the frequency response is extracted, the order of the transfer function can be carefully selected to avoid an overparameterized model. Multiinput/multioutput frequency-response methods are suitable for extracting a transfer matrix which includes the important coupling effects. Finally, the extracted models are driven with the flight-test-control inputs to verify the time-domain response characteristics.

The frequency-domain identification procedure has been applied to an XV-15 tilt-rotor aircraft, a Bell-214-ST single-rotor helicopter, and the NASA/Army CH-47B tandem-rotor research helicopter. The results are briefly described below.

Frequency-Domain Identification of the XV-15- The frequency-domain identification was initiated in 1983 and completed in 1986. The objectives were to identify and document the open-loop dynamics of the XV-15 from flight tests for several

operating conditions including hover, to compare the aircraft and simulation response characteristics for identifying problem areas in the math modeling, and to develop a validated transfer-function model description for future use in control-system studies. The results for hovering flight and cruise flight are reported in detail in references 86 and 85.

Figure 29 shows an example of a comparison of the frequency responses, extracted from flight and simulator data, of the open-loop roll rate response to lateral control input in hovering flight. The correlation of the VMS simulation and the flight data is quite good for the frequency range from 1.0 to 10.0 rad/sec, which indicates that the roll-response control effectiveness is accurately modeled. However, considerable discrepancies are apparent in the math model for the low-frequency-magnitude response. The low-frequency phase comparison suggests that the damping ratio of the unstable roll mode is slightly overestimated by the simulation model (i.e., more unstable), whereas the natural frequency is accurate. Incidentally, these low-frequency errors in the simulation model were also reported during the pilot's qualitative evaluation on the simulator.

Subsequent analysis of the real-time math model indicated problems in the representation of rotor flapping for large lateral-velocity changes (such as the case of the low frequency range of the roll response). There is also strong sensitivity of the numerically linearized transfer functions to the size of perturbation. Corrections to the math modeling in these two areas were included later in the nonreal-time XV-15 simulation. The comparison between the current nonreal-time model, real-time model, and the flight data is shown in figure 29, and indicates the significant improvements achieved during the last 3 years.

Having completed the extraction of the frequency responses, the next step is to fit the frequency response with a transfer-function model. A standard fourth-order model with an effective time-delay term was chosen (ref. 86) as the structure of the model for identification of its attendant parameters. Figure 30 shows a fit of the magnitude and phase of the identified transfer function. The predictive capability of the transfer-function model is illustrated in figure 31, which shows the roll-rate response of the open-loop aircraft to a step aileron input. When the identified transfer function is driven with the same input, the response coplotted in the dashed curve is obtained, which shows the model and flight data responses generally compare very well, and thus provides a validation for the identified model.

Demonstration of Frequency-Sweep Testing Technique Using a Bell 214-ST Helicopter- Research supporting the development of the LHX-handling-qualities specification ADS-33 (ref. 97), which is an updated version of MIL-H-8501A, indicates the need for frequency-domain descriptions to adequately characterize the transient angular-response dynamics of highly augmented combat rotorcraft. The proposed LHX criteria for short-term angular response are given in terms of two frequency-domain parameters--bandwidth (ω_{BW}) and phase delay (τ_p). These quantities are determined directly from frequency response plots of the on-axis angular responses to control inputs, such as was generated from the XV-15 (fig. 29). A key concern in incorporating such descriptions in a specification is the practical problem of extracting frequency responses from flight data for compliance testing.

To address this and other concerns associated with the practicality of using frequency-sweep testing technique, a flight-test demonstration program (6 flight hours) was conducted in October 1985 using an instrumented Bell-214-ST helicopter (fig. 32). Frequency-sweep and step-input tests were performed in hover and cruise (90 knots) for each control axis. The data were then analyzed using the frequency-domain identification procedure described previously. Excellent identification of the frequency responses was achieved for all axes at both flight conditions. As an example, the extracted response of pitch attitude to longitudinal cyclic stick is shown for the hover flight condition in figure 33. An accurate spectral estimate is achieved over a broad frequency range (0.2-10.0 rad/sec), and the required specification compliance parameters are readily obtained. Additional analyses were conducted to identify transfer function models for each axis. These models accurately predict the large-amplitude step response behavior and validate the linearized frequency-response concept for single-rotor helicopters.

Identification of CH-47B Vertical Dynamics Model in Hover- The same frequency-domain procedure that was used in the identification of the two aircraft was also applied to the identification of the vertical dynamics of the CH-47B research aircraft in hover. The objective of this work was to identify the helicopter vertical dynamics for correlation with those developed from the analytical modeling efforts (ref. 50).

Frequency-sweep inputs in collective pitch were employed to identify the frequency response of the vertical acceleration to collective input. The extracted frequency response (fig. 34) indicates that there is a resonant peak at around 17 rad/sec and a substantial phase lead as previously predicted in the analytical study (ref. 49). Based on the analytical modeling efforts, a series of parametric transfer-function models, ranging from first to fifth order was fit to the identified frequency plots. The first-order model corresponds to the classical quasi-static model, and the fourth-order model includes the effects of flapping and inflow dynamics (the fifth-order was used to account for possible effects caused by variation in rotor rpm). The frequency-response fits for a fitst- and a fourth-order model are shown in figure 34. For the first-order quasi-static model, it proved to be difficult to fit the model accurately over the entire frequency range; the fit was therefore limited to the range of 0.1 to 3 rad/sec instead of 0.1 to 20 rad/sec as applied to all of the other models. This causes the first-order model to match the flight data better at low frequency than the higher-order models (fig. 34). All of the higher-order models exhibit a nonminimum phase characteristic as predicted in the analytical modeling efforts (ref. 49).

As a means for testing the predictive capability of the identified models, the vertical responses to a step input in collective input were generated from the models. These responses compare favorably with those of the analytical model. Some of the responses of the identified models are plotted together with flight data as shown in figure 35. As expected, the first-order models, because of the limited frequency range of applicability, fails completely to predict the overshoot of the vertical acceleration owing to the high-order effects of inflow and flapping

dynamics. The fourth-order model provides a much better predictive capability than does the first-order model for the initial transient.

CONCLUDING REMARKS

This paper has reviewed the progress made in joint NASA/Army research concerning rotorcraft flight-dynamics modeling, flight control design methodologies, and parameter identification. These interactive research disciplines all require attention in order to provide a basis for exploring analytically and experimentally the handling qualities implications of a variety of dynamic concepts aimed at assisting the pilot in performing a required mission. Although this integrated approach to the research is probably required for all classes of aircraft, the need is particularly acute for rotorcraft because of their mathematical complexity, high-order dynamic characteristics, and demanding mission requirements. Accordingly, the results that have been reviewed here form the basis for combined research efforts which are currently under way to integrate dynamics, controls, and identification methodologies.

The need for this integration is apparent from most of the work reviewed here. As was reviewed in the paper, the research on real-time simulation models has led to a capability of including rigid blade flapping modes, initially for the rotor disk and more recently using blade element models. These models have been appropriate for the types of missions considered to date, but must be extended for missions which require more pilot-aircraft performance to include the important effects of additional degrees of freedom such as lag or elastic modes while retaining adequate simplicity for design and simulation purposes. Further, the models must be accurate over greater regions of the flight envelope; the work described in the paper for high-g maneuvering forms the basis for more accurate full-flight-envelope design tools. To ascertain the importance of the higher-order terms, parameter identification techniques must be integrated into the modeling process, using flight data as the verification standard. In particular, the frequency-domain procedures developed at NASA and discussed in this paper are excellently suited to assessing the influence of these dynamics and providing a rational basis for the selection of lower-order models.

It is also clear from the joint work reviewed here that these higher order dynamics must be accounted for explicitly early in the design process, regardless of their origin. The flight experiments demonstrated the importance for modern control applications of rotor dynamics and also aerodynamic (inflow) dynamics; the high-gain, model-following system that has been developed and demonstrated has utilized models that are accurate to higher frequencies to achieve improved control system performance. Equally important, the control system implementation itself adds dynamics that have historically been overlooked in rotorcraft control designs; the review of an existing rotorcraft digital-control-system design and implementation showed that current practices do not account sufficiently for the digital design details and that the achievable control system performance remains far less than was

predicted. Therefore, in general, the work conducted in the past 10 yr has inevitably pointed to the need for models and methodologies accurate over higher frequency ranges and capable of dealing explicitly with a variety of interactive effects, and, as demonstrated in this paper, the research has become increasingly oriented in this direction.

The current NASA/Army research for rotorcraft flight dynamics and controls is oriented to examining concepts that require even higher gains and more interaction among the controls and the various dynamics of the rotorcraft systems, and hence may be said to be becoming more closely coupled to the actual details of the rotor-craft. The need for this closer coupling to the details of the rotorcraft stems from the increasing emphasis on demanding rotorcraft missions such as air-to-air combat and automated nap-of-the-Earth flight. To achieve the requisite improvements in agility and maneuverability, a variety of interactive elements must be considered in the modeling and control design process; such elements include integrated flight/propulsion control, rotor state control, high bandwidth stability/control augmentation, rotor-rpm energy transfer, higher harmonic control, and envelope limiting and cueing. As the review of previous work presented in this paper has shown, a considerable extension of existing knowledge and techniques is required to perform the integration of all of these elements. The goal is to provide systematic modeling and design procedures capable of dealing with these new problems, and to integrate the technologies that have been initiated in the joint research of the past 10 years.

REFERENCES

1. Talbot, P. D.; Tinling, B. E.; Decker, W. A.; and Chen, R. T. N.: A Mathematical Model of a Single Main Rotor Helicopter for Piloted Simulation. NASA TM-84281, Sept. 1982.

2. Chen, R. T. N.: A Simplified Rotor System Mathematical Model for Piloted Flight Dynamics Simulation. NASA TM-78575, 1979.

3. Chen, R. T. N.: Effects of Primary Rotor Parameters on Flapping Dynamics. NASA TP-1431, Jan. 1980.

4. Decker, W. A.; Adam, C. F.; and Gerdes, R. M.: Model Development and Use of Simulators for Investigating Autorotation. Paper FAA Conf. on Helicopter Simulation, Atlanta, GA, Apr. 1984.

5. Decker, W. A.; Adam, C. F.; and Gerdes, R. M.: Pilot Use of Simulator Cues for Autorotation Landing. 1986 AHS Forum, Washington, DC, June 1986.

6. Sheridan, P. F.; Robinson, C.; Shaw, J.; and White, F.: Mathematical Modeling for Helicopter Simulation of Low speed, Low Altitude, and Steeply Descending flight. NASA CR-166385, 1982.

7. Chen, R. T. N.: Selection of Some Rotor Parameters to Reduce Pitch-Roll Coupling of Helicopter Flight Dynamics. Preprint no. I-6, National Specialists' Meeting, Rotor System Design, AHS Mideast Region, Philadelphia, Oct. 1980.

8. Chen, R. T. N.; and Talbot, P. D.: An Exploratory Investigation of the Effects of Large Variations in Rotor System Dynamics Design Parameters on Helicopter Handling Qualities in NOE Flight. J. AHS, July 1978, pp. 23-36.

9. Lewis, M. S.; and Aiken, E. W.: Piloted Simulation of One-on-One Helicopter Air Combat at NOE Flight Levels. NASA TM-86686, Apr. 1985.

10. Lewis, M. S.: A Piloted Simulation of One-on-One Helicopter Air Combat in Low Level Flight. J. AHS, vol. 31, no. 2, Apr. 1986, pp. 19-26.

11. Lebacqz, J. V.; and Forrest, R. D.: Control Position Gradient and Stability/Control Augmentation Effects on Helicopter Handling Qualities for Instrument Approach. J. AHS, Jan. 1982, pp. 35-41.

12. Lebacqz, J. V.; Chen, R. T. N.; Gerdes, R. M.; and Weber, J. M.: A summary of NASA/FAA Experiments Concerning Helicopter IFR Airworthiness Criteria. J. AHS, July 1983, pp. 63-70.

13. Lebacqz, J. V.: Ground Simulation Investigation of Helicopter Decelerating
    Instrument Approaches. J. Guidance, Control, and Dynamics, vol. 6, no. 5,
    Sept./Oct. 1983, pp. 330-338.

14. Curtiss, H. C., Jr.; Sun, M.; and Putman, W. F.: Rotor Aerodynamics in Ground
    Effect at Low Advance Ratios. Paper 81-5, 37th Annual Forum of the AHS, New
    Orleans, LA, May 1981.

15. Curtiss, H. C., Jr.; Sun, M.; and Hanker, E. J.: dynamic Phenomena in Ground
    Effect. Paper A-83-39-76-000, 39th Annual Forum of the AHS, May 1983.

16. Curtiss, H. C., Jr.; Erdman, W.; and Sun, M.: Ground Effect Aerodynamics.
    Paper presented at the International Conf. on Rotorcraft Basic Research,
    Triangle Part, NC, Feb. 19-21, 1985.

17. Lewis, M. S.; Mansur, M. H.; and Chen, R. T. N.: A simulator Investigation of
    Parameter Affecting Helicopter Handling Qualities in Air Combat. AHS
    National Forum, St. Louis, MO, May 1987.

18. Hilbert, K. B.: A Mathematical Model of the UH-60A Helicopter. NASA TM-85890,
    Apr. 1984.

19. Landis, K. H.; and Glusman, S. I.: Development of ADOCS Controllers and Con-
    trol Laws. NASA CR-177339, March 1985.

20. Jewell, W. F.; Clement, F. W.; and Johns, J. B.: Real Time Piloted Simulation
    Investigation of Helicopter Flying Qualities During Approach and Landing on
    Nonaviation Ships. AIAA Paper 86-0490, Jan. 1986.

21. Bouwer, G.; and Hilbert, K. B.: A Piloted Simulator Investigation of Decou-
    pling Helicopters Using a Model-Following Control System. AHS Annual Forum,
    May 1984.

22. Aiken, E. W.: A Mathematical Representation of an Advanced Helicopter for
    Piloted Simulator Investigations of Control-System and Display Variations.
    NASA TM-81203, July 1980.

23. Aiken, E. W.; and Merrill, R. K.: Results of a Simulator Investigation of
    Control System and Display Variations for an Attack Helicopter Mission.
    36th Annual AHS Forum, Washington, DC, May 1980.

24. Aiken, E. W.; and Blanken, C. L.: Piloted Simulation of the YAH-64 Backup
    Control System Engagement. NASA TM-81293 (USAAVRADCOM TR-81-A-11), July
    1981.

25. Bivens, C. C.: Directional Handling Qualities Requirements for Nap-of-the-
    Earth Tasks. J. AHS, vol. 31, no. 1, Jan. 1986, pp. 37-42.

26. Talbot, P. D.; and Corliss, L. D.: A Mathematical Force and Moment Model of a UH-1H Helicopter for Flight Dynamics Simulations. NASA TM-73254, June 1977.

27. Baker, F. A.; Janes, D. N.; Corliss, L. D.; Liden, S.; Merrick, B.; and Dugan, D. C.: V/STOLAND Avionics System Flight Test Data on a UH-1H Helicopter. NASA TM-78591, Feb. 1980.

28. Corliss, L. C.; and Talbot, P. D.: A Failure Effects Simulation of a Low Authority Flight Control Augmentation System on a UH-1H Helicopter. NASA TM-73258, 1977.

29. Hackett, W. E., Jr.; Gernett, T. S., Jr.; and Borek, B. V.: Mathematical Model fo the CH-47B Helicopter Capable of Real-Time Simulation of the Full Flight Envelope. NASA CR-166458, July 1983.

30. Weber, J. M.; Liu, T. Y.; and Chung, W.: A Mathematical Simulation Model of a CH-47B Helicopter. NASA TM-84351, Aug. 1984.

31. Weber, J. M.; et al.: A Lagrange-D'Alembert Formulation of the Equations of Motion of a Helicopter Carrying an Externally Suspended Load. NASA TM-85864, Feb. 1985.

32. Hilbert, K. B.; Lebacqz, J. V.; and Hindson, W. S.: Flight Investigation of a Multivariable Model-Following Control System for Rotorcraft. AIAA Paper 86-9779, AIAA 3rd Flight Test Conf., Las Vegas, April 1986.

33. Holdridge, R. D.; Hindson, W. S.; and Bryson, A. E.: LQG-Design and Flight-Test of a Velocity-Commands System for a Helicopter. Paper presented at AIAA Conf. on Guidance and Control, Snowmass, CO, Aug. 19-21, 1985.

34. Howlett, J. J.: UH-60A Black Hawk Engineering Simulation Program. NASA CR-166309, 1981.

35. Ballin, M. G.: Validation of a Real-Time Engineering Simulation of the UH-60A Helicopter. NASA TM-88359, Feb. 1987.

36. Miheloew, J. R.; and Chen, R. T. N.: Rotorcraft Flight-Propulsion Control Integration. Vertiflite, vol. 30, no. 6, Sept./Oct. 1984, pp. 45-47.

37. Paulk, C. H., Jr.; Astill, D. L.; and Donley, S. T.: Simulation and Evaluation of the 54-2F Helicopter in a Shipboard Environment Using the Interchangeable Cab System. NASA TM-84387, Aug. 1983.

38. Phillips, J. D.: Mathematical Model of the 34-3G Helicopter. NASA TM-84316, Dec. 1982.

39. Howlett, J. J.: RSRA Simulation Model--Vol. I. Mathematical Model Equations. Sikorsky Aircraft, SER-72009 (under contract NASI-13000), Oct. 1974).

40. Harendra, P. B.; et al.: V/STOL Tilt Rotor Study. Vol. V. A Mathematical Model for Real Time Flight Simulation of the Bell Model 301 Tilt Rotor Research Aircraft. NASA CR-114614, 1973.

41. Lebacqz, J. V.; and Scott, B. C.: Ground Simulation Investigation of VTOL Airworthiness Criteria for Terminal Area Operations. AIAA J. GCD, vol. 8, no. 6, Nov./Dec. 1985, pp. 761-767.

42. Etkin, B.: Dynamics of Atmospheric Flight. John Wiley & Sons, Inc., 1972.

43. Seckel, E.: Stability and Control of Airplanes and Helicopters. Academic Press (New York), 1964.

44. General Requirements for Helicopter Flying and Ground Handling Qualities. Specification MIL-H-8501A, Sept. 1961.

45. V/STOL Handling. Part I. Criteria and Discussion. AGARD Report 577, June 1973.

46. Flying Qualities of Piloted V/STOL Aircraft. Specification MIL-F-83300, Dec. 31, 1970.

47. Flying Qualities of Piloted Airplanes. Specification MIL-F-8785B(ASG), 7 Aug. 1969.

48. Chen, R. T. N.; and Hindson, W. S.: Influence of High-Order Dynamics on Helicopter Flight-Control System Bandwidth. AIAA J. Guidance, Control, and Dynamics, vol. 9, no. 2, March/April 1986, pp. 190-197.

49. Chen, R. T. N.; and Hindson, W. S.: Influence of Dynamic Inflow on the Helicopter Vertical Response. NASA TM-88327, June 1986.

50. Chen, R. T. N.: Unified Results of Several Analytical and Experimental Studies of Helicopter Handling Qualities in Visual Terrain Flight. NASA CP-2219, April 1982, pp. 59-74.

51. Chen, R. T. N.; and Tischler, M. B.: The Role of Modeling and Flight Testing in Rotorcraft Parameter Identification. Presented at the 1986 AHS Forum, Washington, DC, June 1986.

52. Chen, R. T. N.: Kinematic Properties of Rotary-Wing and Fixed-Wing Aircraft in Steady Coordinated High-g Turns. AIAA Paper 81-1855, Aug. 1981.

53. Chen, R. T. N.: Kinematic Properties of Rotary-Wing and Fixed-wing Aircraft in Steady Coordinated High-g Turns. AIAa Paper 81-1855, Aug. 1981.

54. Chen, R. T. N.; and Jeske, J. A.: Influence ofSideslip on the Helicopter in Steady Coordinated Turns. J. AHS, Oct. 1982, pp. 84-92.

55. Chen, R. T. N.: Flight Dynamics of Rotorcraft in Steep High-g Turns. J. Aircraft, vol. 21, no. 1, Jan. 1984, pp. 14-22.

56. Chen, R. T. N.: Efficient Algorithms for Computing Trim and Small-Disturbance Equations of Motion of Aircraft in Coordinated and Uncoordinated, Steady, Steep Turns. NASA TM-84324, Feb. 1983.

57. Chen, R. T. N.; Jeske, J. A.; and Steinberger, R. H.: Influence of Sideslip on the Flight Dynamics of Rotorcraft in Steep Turns at Low Speeds. AHS 39th Annual Forum, St. Louis, MO, May 1983.

58. Houston, S. S.: On the Analysis of Helicopter Flight Dynamics During Maneuvers. Paper 80, 11th European Rotorcraft Forum, 10-13 Sept. 1985, London.

59. Padfield, G. D.: On the Use of Approximate Models in Helicopter Flight Mechanics. Vertica, vol. 5, 1981, pp. 243-259.

60. Briczinski, S. J.; and Cooper, D. E.: Flight Investigation of Rotor/Vehicle State Feedback. NASA CR-132546, Jan. 1975.

61. Landis, K. H.; and Aiken, E. W.: Simulator Investigations of Side-Stick Controller/Stability and Control Augmentation Systems for Night Nap-of-the-Earth Flight. J. AHS, Jan. 1984, pp. 56-65.

62. McRuer, D.; Johnson, D.; and Meyers, T.: A Perspective on Superaugmented Flight Control Advantages and Problems. AGARD Conference on Active Control, Ontario, Canada, 1984.

63. Ormistron, R. A.: Application of Simplified Inflow Models to Rotorcraft Dynamic Analysis. J. Am. Helicopter Sci., July 1976, pp. 34-37.

64. Johnson, W.: Influence of Unsteady Aerodynamics on Hingeless Rotor Ground Resonance. J. Aircraft, vol. 19, 1982, pp. 668-673.

65. Friedmann, P. P.; and Venkatesan, C.: Influence of Various Unsteady Aerodynamic Models on the Aeromechanical Stability of a Helicopter in Ground Resonance. NASA CP-2400, 1985, pp. 207-218.

66. Gaonkar, G. H.; and Peters, D.: A Review of Dynamic Inflow and Its Effect on Experimental Correlations. NASA CP-2400, 1985, pp. 187-203.

67. Pitt, D. M.; and Peters, D. A.: Theoretical Prediction of Dynamic-Inflow Derivatives. J. Vertica, vol. 5, 1981, pp. 21-34.

68. Carpenter, P. J.; and Fridovich, B.: Effect of a Rapid-Pitch Increase on the Thrust and Induced-Velocity Response of a Full-Scale Helicopter Rotor. NACA TN-3044, 1953.

69. Curtiss, H. C., Jr.: Stability and Control Modelling. Paper 41, 12th European Rotorcraft Forum, Sept. 1986, Garmisch-Partenhirchen, Germany.

70. Mihaloew, J.; Ballin, M. G.; and Ruttledge, D. C. G.: Rotorcraft Flight-Propulsion Control Integration. Paper 1987 NASA/Army Rotorcraft Technology Conference, 1987.

71. Landis, K. H.; Dunford, P. J.; Aiken, E. W.; and Hilbert, K. B.: Simulator Investigation of Side-Stick Controller/Stability and Control Augmentation Systems for Helicopter Visual Flight. J. AHS, vol. 30, no. 2, April 1985, pp. 3-13.

72. Aiken, E. W.; Hilbert, K. B.; Landis, K. H.; and Glusman, S. I.: An Investigation of Side-Stick Controller/Stability and Control Augmentation System Requirements for Helicopter Terrain Flight Under Reduced Visibility Conditions. AIAA Paper 84-0235, Jan. 1984.

73. Brigadier, W. L.: Analysis of Control Actuator Authority Requirements for Attitude and Translational Rate Command Augmentation Systems for the XV-15 Tilt Rotor Research A/C. NASA TM-81243, Dec. 1980.

74. Tischler, M. B.: Pigtail Control of Highly Augmented Combat Rotorcraft. NASA TM-88346, 1987.

75. Lebacqz, J. V.; and Chen, R. T. N.: Design and Flight Test of a Decoupled Velocity Control System for VTOL Landing Approach. AIAA/AFM Conf., Aug. 1977.

76. Miyajima, K.: An Analytical Design of a High Performance Stability and Control Augmentation System for a Hingeless Rotor Helicopter. J. AHS, July 1979, pp. 29-35.

77. Ly, U. L.: A Design Algorithm for Robust Low-Order Controllers. Report 536, Stanford Univ., Stanford, CA, Nov. 1982.

78. Hilbert, K. B.; and Bouwer, G.: The Design of a Model-following Control System for Helicopters. AIAA G. and C. Conf., Seattle, WA, 1984.

79. Townsend, B. K.: The Application of Quadratic Optimal Cooperative Control Synthesis to a CH-47 Helicopter. 1986 AHS Lichten Award Paper, NASA TM-88353, Sept. 1986.

80. Parameter Estimation Techniques for Applications in Aircraft Flight Testing. NASA TN D-7647, April 1974.

81. Methods for Aircraft State and Parameter Identification. AGARD-CP-172, Nove. 1974.

82. Parameter Identification. AGARD-LS-104, Nov. 1979.

83. Tomaine, R. L.: Flight Data Identification of Six Degree-of-Freedom Stability and Control Derivatives of a Large "Crane" Type Helicopter. NASA TM X-73958, Sept. 1976.

84. Hall, W. W., Jr.; Bohn, J. G.; and Vincent, J. H.: Development of Advanced Techniques for Rotorcraft State Estimation and Parameter Identification. NASA CR-159297, Aug. 1980.

85. Tischler, M. B.: Frequency Response Identification of XV-15 Tilt-Rotor Aircraft Dynamics. Ph.D. Dissertation, Stanford Univ., Stanford, CA, 1987.

86. Tischler, M. B.; Leung, J. G. M.; and Dugan, D. C.: Frequency-Domain Identification of XV-15 Tilt-Rotor Aircraft Dynamics in Hovering Flight. AIAA Paper 83-2695 (also in condensed version in J. Amer. Helicopter Soc., vol. 30, no. 2, Apr. 1985, pp. 38-48).

87. Tischler, M. B.; and Kaletka, J.: Modeling XV-15 Tilt-Rotor Aircraft Dynamics by Frequency and Time-Domain Identification Techniques. AGARD Paper 9, Oct. 1986.

88. Gould, D. G.; and Hindson, W. S.: Estimates of the Stability Derivatives of a Helicopter and a V/STOL Aircraft from Flight Data. AGARD-CP-172, Nov. 1974.

89. Molusis, J. A.: Helicopter Stability Derivative Extraction from Flight Data Using a Bayesian Approach to Estimation. J. Amer. Helicopter Soc., July 1973.

90. Molusis, J. A.: Rotorcraft Derivative Identification from Analytical Models and Flight Test Data. AGARD-CP-172, Nov. 1974.

91. Tomaine, R. L.; Bryant, W. H.; and Hodge, W. F.: VALT Parameter Identification Flight Test. European Rotorcraft Paper 73, Sept. 1978.

92. DuVal, R. W.; and Mackie, D. B.: Identification of a Linear Model at Rotor-Fuselage Dynamics from Nonlinear Simulation Data. Proceedings of the 6th European Rotorcraft and Powered Lift Aircraft Forum, Bristol, England, 1980.

93. DuVal, R. W.; Wang, J. C.; and Demiroz, M.: A Practical Approach to Rotorcraft System Identification. Proceeding of 39th American Helicopter Society Forum, 1983.

94. Padfield, G. D.; and DuVal, R. W.: Application of Parameter Estimation Methods to the Prediction of Helicopter Stability, Control, and Handling Characteristics. Proceedings of the NASA/American Helicopter Society Specialists Meeting on Helicopter Handling Qualities, NASA CP-2219, 1982.

95. Kaletka, J.: Rotorcraft Identification Experience. AGARD-LS-104, Nov. 1979, pp. 7-1 to 7-32.

96. Kaletka, J.: Practical Aspects of Helicopter Parameter Identification. AIAA CP849, AIAA Paper 84-2081, 1984, pp. 112-122.

97. Hoh, R. H.; Mitchell, D. G.; Ashkenas, I. L.; Aponso, B. L.; Ferguson, S. W.; Rosenthal, T. J.; Key, D. L.; and Blanken, C. L.: Proposed Airworthiness Design Standard: Handling Qualities Requirements for Military Rotorcraft. System Technology, Inc. TR-1194-2, 20 Dec. 1985.

TABLE 1.– ROTORCRAFT MATH MODELS FOR PILOT-IN-THE-LOOP SIMULATION

Applications	Model complexity							
	Linear aerodynamics with simplifications					Nonlinear aerodynamics		
	Fuselage and quasi-static rotor 6 DOF	Fuselage and rotor flap 9 DOF	Fuselage and rotor flap/rpm 10 DOF	Fuselage and rotor flap/lag 12 DOF	Fuselage and rotor flap/lag/ 16 DOF	Fuselage and quasi-static rotor 6 DOF	Fuselage and rotor flap/rpm 10 DOF	Fuselage and rotor flap/lag/ pitch/rpm 16 DOF
General handling qualities--well within flight envelope								
Basic aircraft								
Low frequency maneuvers	X							
High frequency maneuvers		X	X					
SCAS research								
Fuselage feedback	X	X						
Fuselage/rotor feedback		X	X	X	X			
General handling qualities--full flight envelope								
Basic aircraft								
Envelope exploration and maneuvering performance						X	X	X
Boundary limiting and expanding SCAS							X	X
Specific aircraft handling qualities						X	X	X

TABLE 2.- ALGORITHMS FOR COMPUTING TRIM CONDITIONS FOR A ROTORCRAFT IN A STEADY, UNCOORDINATED FLIGHT

A. Steady Uncoordinated Turns

Steady-state Euler equations

$$n_x - \sin \Theta - \tan \phi_1 (\sin \alpha \cos \beta \cos \Theta \sin \Phi - \sin \beta \cos \Theta \cos \Phi) = 0$$

$$n_y + \cos \Theta \sin \Phi - \tan \phi_1 \cos \beta (\cos \alpha \cos \Theta \cos \Phi + \sin \alpha \sin \Theta) = 0$$

$$n_z + \cos \Theta \cos \Phi + \tan \phi_1 (\sin \beta \sin \Theta + \cos \alpha \cos \beta \cos \Theta \sin \Phi) = 0$$

$$L + I_{yz}(q^2 - r^2) + I_{xz}pq - I_{xy}rp + (I_y - I_z)qr = 0$$

$$M + I_{xz}(r^2 - p^2) + I_{xy}qr - I_{yz}pq + (I_z - I_x)rp = 0$$

$$N + I_{xy}(p^2 - q^2) + I_{yz}rp - I_{xz}qr + (I_x - I_y)pq = 0$$

$$\phi_1 = \tan^{-1}\left(\frac{\dot{\Psi}V}{g}\right)$$

$$= \pm \tan^{-1}\left[\frac{(n^2 - 1)^{1/2}}{\cos \gamma}\right], \quad + \text{ right turn; } - \text{ left turn}$$

$$n^2 = n_x^2 + n_y^2 + n_z^2$$

Kinematic relationships

$$q = \dot{\Psi} \sin^2\phi_1 \left\{ - (\sin \gamma \sin \beta + n_y \cot^2\phi_1) \right.$$

$$\left. \pm \left[(\sin \gamma \sin \beta + n_y \cot^2\phi_1)^2 - \frac{1}{\sin^2\phi_1}(\sin^2\gamma - \cos^2\beta + n_y^2 \cot^2\phi_1)\right]^{1/2} \right\}$$

$$q \geq 0$$

$$r' = \frac{q + \dot{\Psi}n_y}{\tan \phi_1 \cos \beta}$$

$$p' = - \frac{\dot{\Psi} \sin \gamma}{\cos \beta} - q \tan \beta$$

$$p = p' \cos \alpha - r' \sin \alpha$$

$$r = p' \sin \alpha + r' \cos \alpha$$

$$\Theta = \sin^{-1}(-p/\dot{\Psi})$$

$$\Phi = \tan^{-1}(q/r)$$

B. Steady Uncoordinated Straight Flight

Steady-state Euler equations $\quad n_x - \sin \Theta = 0 \qquad n_z + \cos \Theta \cos \Phi = 0$

$$n_y + \cos \Theta \sin \Phi = 0 \qquad\qquad L = M = N = 0$$

Kinematic relationships $\qquad p = q = r = 0$

$$\Theta = \sin^{-1}\left\{\frac{\cos \alpha(\sin \gamma - n_y \sin \beta) + \sin \alpha[\cos^2\beta - \sin^2\gamma + n_y(2 \sin \beta \sin \gamma - n_y)]^{1/2}}{\cos \beta}\right\}$$

$$\Phi = \sin^{-1}\left(\frac{-n_y}{\cos \Theta}\right)$$

TABLE 3.- SMALL-PERTURBATION EQUATIONS OF MOTION OF AIRCRAFT FROM STEADY TURNING FLIGHT (ACCELERATION DERIVATIVES NEGLECTED)

$$\dot{x} = Fx + G\underline{u}$$

$$x \triangleq (\delta u,\ \delta w,\ \delta q,\ \delta\theta;\ \delta v,\ \delta p,\ \delta\phi,\ \delta r)^T$$

$$\underline{u} \triangleq (\Delta\delta_e,\ \Delta\delta_c,\ \Delta\delta_a,\ \Delta\delta_p)^T$$

$$F = \begin{bmatrix}
x_u & x_w - q_0 & x_q - w_0 & -g\cos\Theta_0 & x_v + r_0 & x_p & 0 & x_r + v_0 \\
z_u + q_0 & z_w & z_q + u_0 & -g\cos\phi_0\sin\Theta_0 & z_v - p_0 & z_p - v_0 & -g\sin\phi_0\cos\Theta_0 & z_r \\
m_u & m_w & m_q & 0 & m_v & m_p - 2p_0\frac{I_{xz}}{I_y} - r_0\frac{(I_x - I_z)}{I_y} & 0 & m_r + 2r_0\frac{I_{xz}}{I_y} - p_0\frac{(I_x - I_z)}{I_y} \\
0 & 0 & \cos\phi_0 & 0 & 0 & 0 & -\dot\psi_0\cos\Theta_0 & -\sin\phi_0 \\
y_u - r_0 & y_w + p_0 & y_q & -g\sin\phi_0\sin\Theta_0 & y_v & y_p + w_0 & g\cos\phi_0\cos\Theta_0 & y_r - u_0 \\
\ell'_u & \ell'_w & \ell'_q + t_1 p_0 - t_2 r_0 & 0 & \ell'_v & \ell'_p + t_1 q_0 & 0 & \ell'_r - t_2 q_0 \\
0 & 0 & \sin\phi_0\tan\Theta_0 & \dot\psi_0\sec\Theta_0 & 0 & 1 & 0 & \cos\phi_0\tan\Theta_0 \\
n'_u & n'_w & n'_q - t_3 p_0 - t_1 r_0 & 0 & n'_v & n'_p - t_3 q_0 & 0 & n'_r - t_1 q_0
\end{bmatrix}$$

$$G = \begin{bmatrix}
x_{\delta_e} & x_{\delta_c} & x_{\delta_a} & x_{\delta_p} \\
z_{\delta_e} & z_{\delta_c} & z_{\delta_a} & z_{\delta_p} \\
m_{\delta_e} & m_{\delta_c} & m_{\delta_a} & m_{\delta_p} \\
0 & 0 & 0 & 0 \\
y_{\delta_e} & y_{\delta_c} & y_{\delta_a} & y_{\delta_p} \\
\ell'_{\delta_e} & \ell'_{\delta_c} & \ell'_{\delta_a} & \ell'_{\delta_p} \\
0 & 0 & 0 & 0 \\
n'_{\delta_e} & n'_{\delta_c} & n'_{\delta_a} & n'_{\delta_p}
\end{bmatrix}$$

where

$$\left. \begin{aligned} x_i &= \frac{X_i}{m}\ ;\quad y_i = \frac{Y_i}{m}\ ;\quad z_i = \frac{Z_i}{m} \\[4pt] m_i &= \frac{M_i}{I_y} \end{aligned} \right\} \qquad i = u,\ v,\ w;\ p,\ q,\ r;\ \delta_e,\ \delta_c,\ \delta_a,\ \delta_p$$

$$\ell'_i = \frac{I_z}{I_x I_z - I_{xz}^2}\, L_i + \frac{I_{xz}}{I_x I_z - I_{xz}^2}\, N_i$$

$$n'_i = \frac{I_{xz}}{I_x I_z - I_{xz}^2}\, L_i + \frac{I_x}{I_x I_z - I_{xz}^2}\, N_i$$

$$t_1 = \frac{I_{xz}(I_z + I_x - I_y)}{I_x I_z - I_{xz}^2}\ ;\qquad t_2 = \frac{I_z(I_z - I_y) + I_{xz}^2}{I_x I_z - I_{xz}^2}\ ;\qquad t_3 = \frac{I_x(I_y - I_x) - I_{xz}^2}{I_x I_z - I_{xz}^2}$$
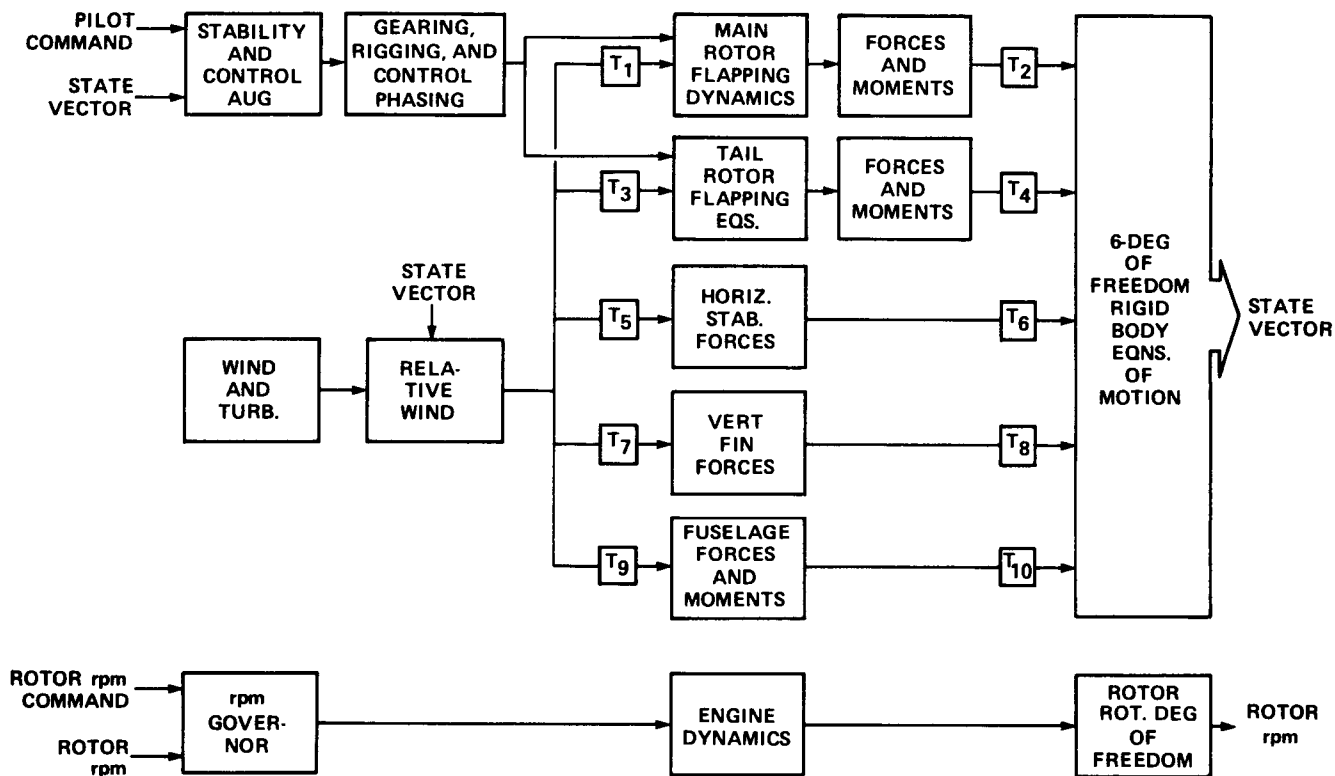
Figure 1.- Block diagram showing principal elements of single rotor helicopter model.
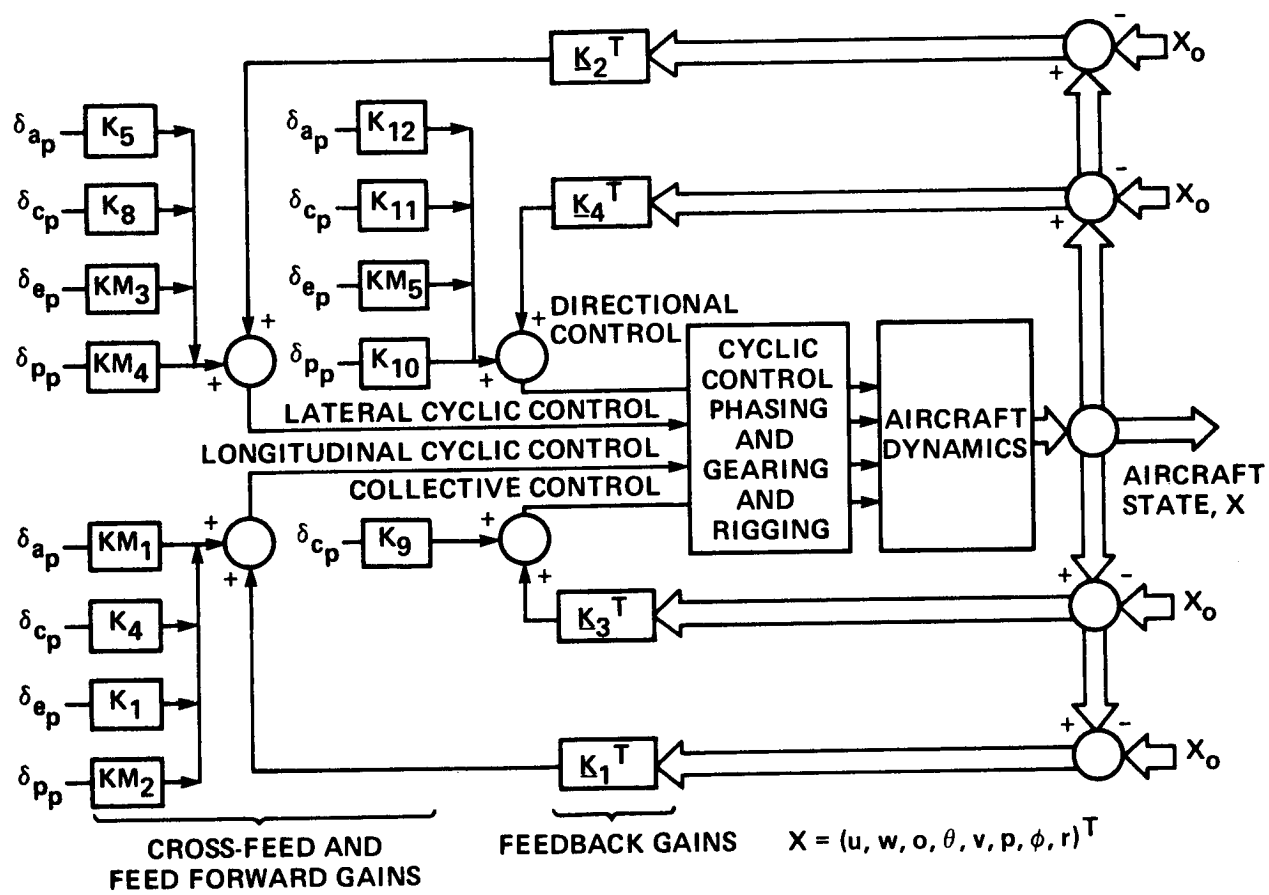
Figure 2.- Structure of control system model.
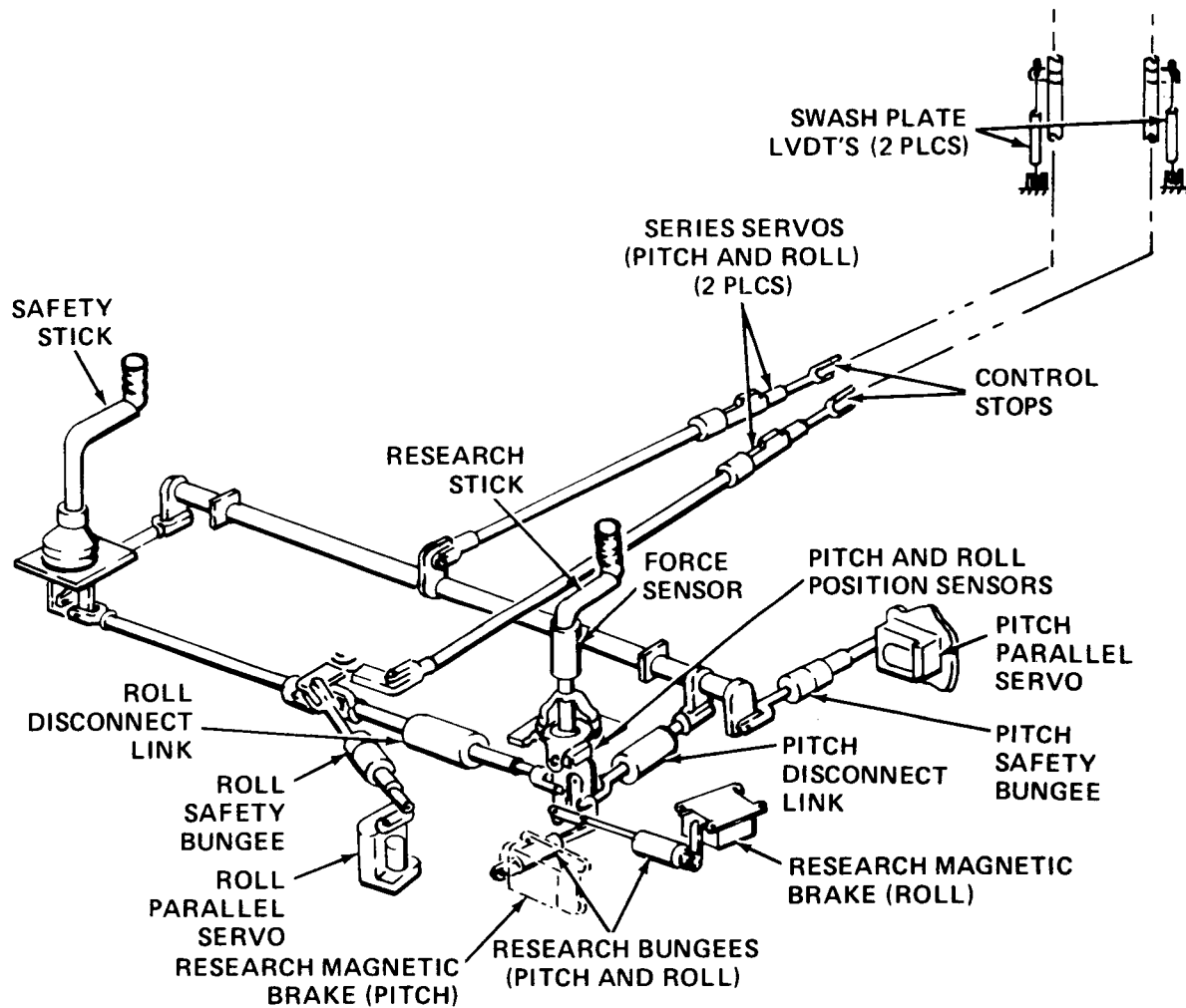
Figure 3.- UH-1H V/STOLAND control system longitudinal and lateral cyclic controls.
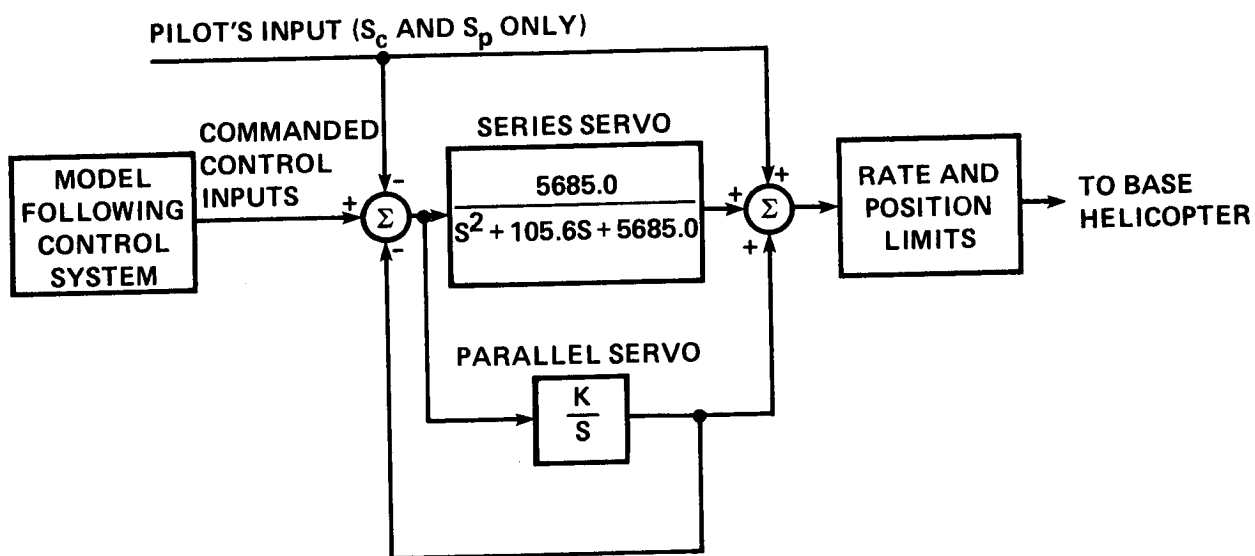
Figure 4.- Simulated UH-1H V/STOLAND actuating system.
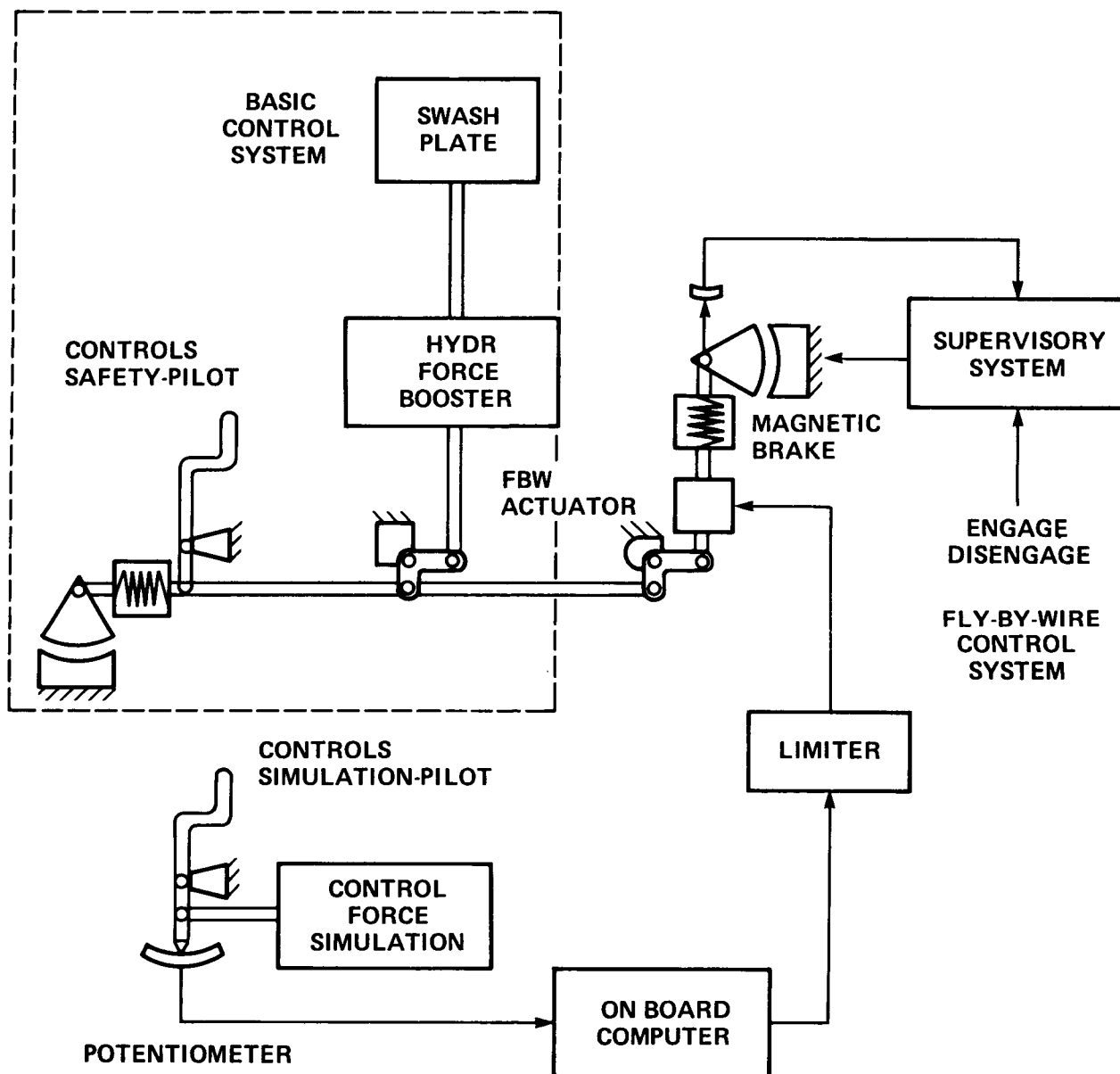
Figure 5.- BO-105 S3 control system.
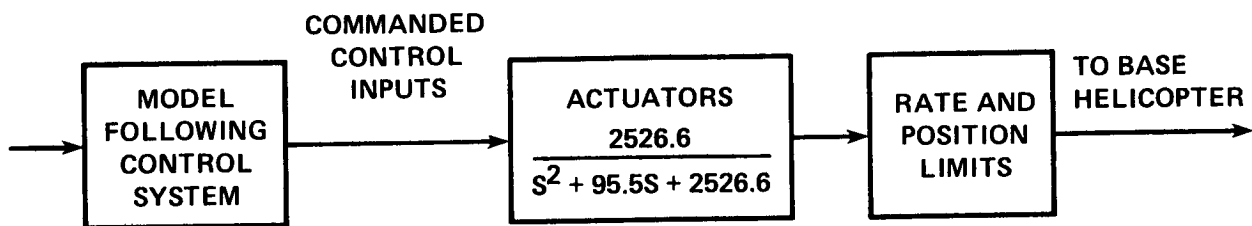
Figure 6.- Simulated BO-105 S3 actuator dynamics.

(a)

(b)
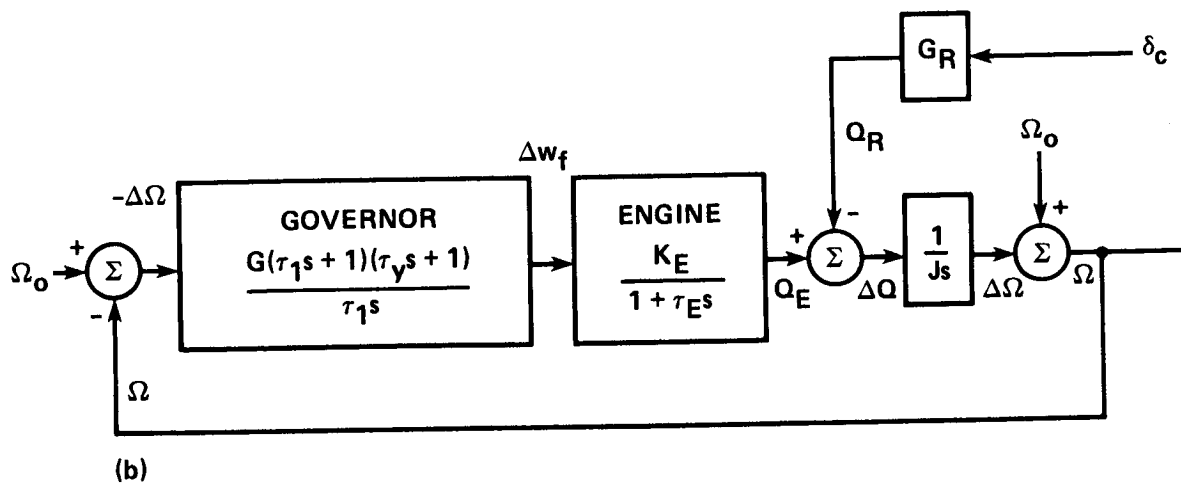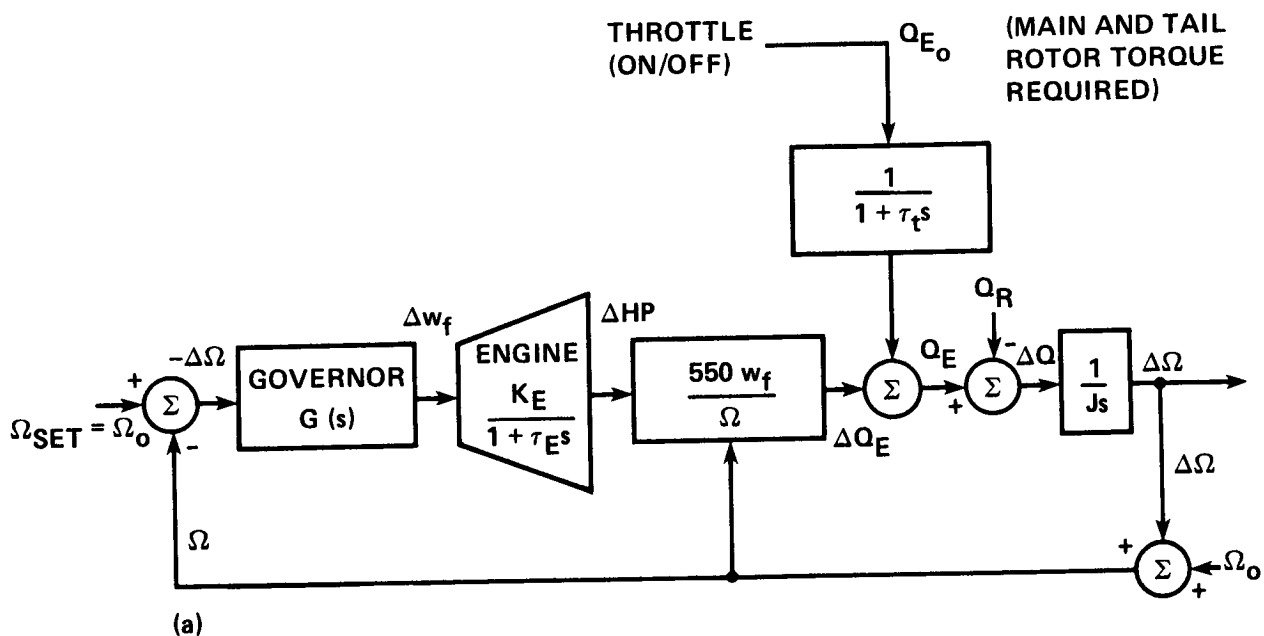
Figure 7.- RPM governor. (a) Generic. (b) Simulated.
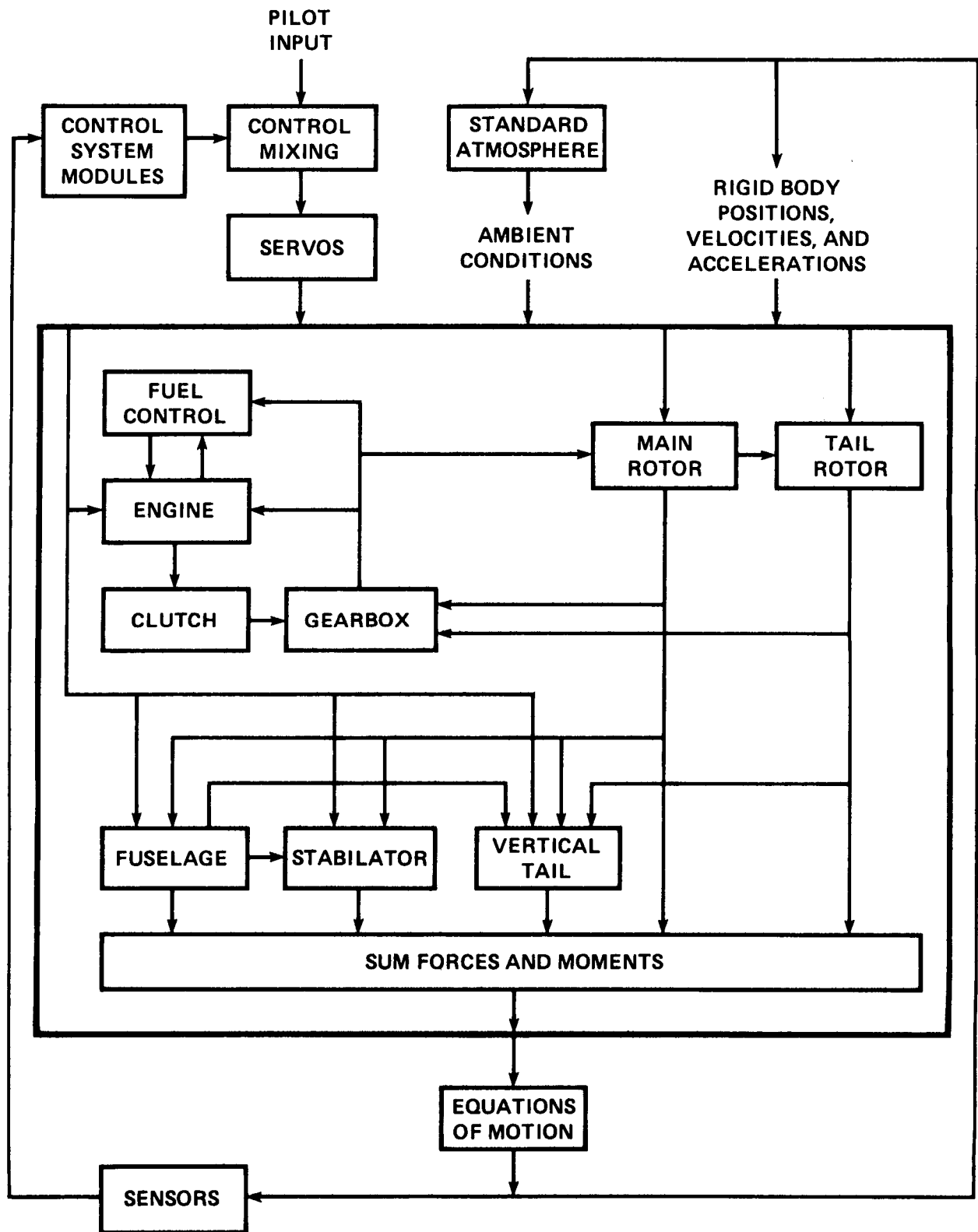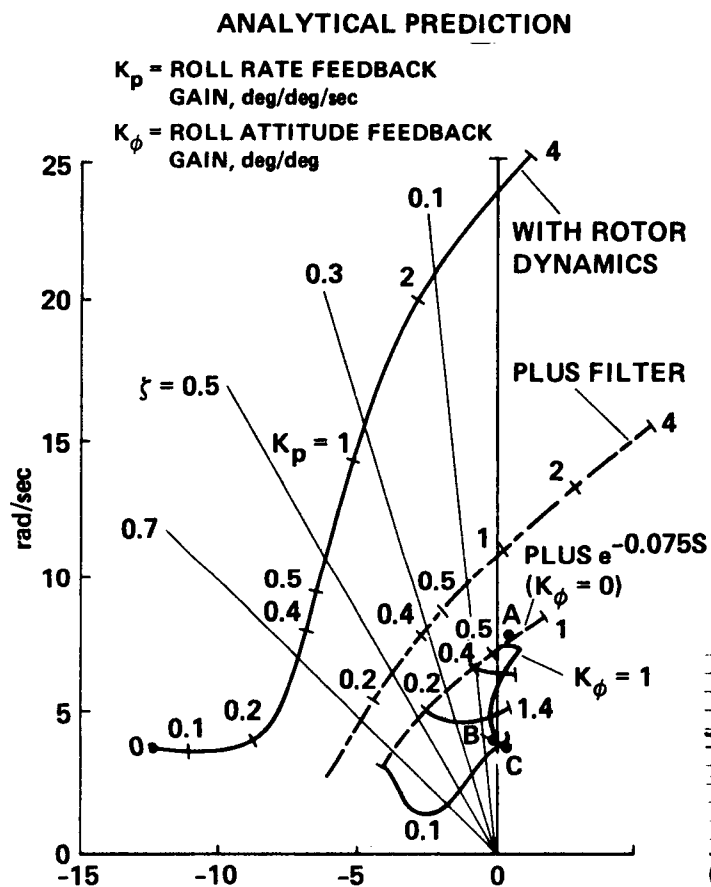
Figure 8.- GenHel simulation elements.
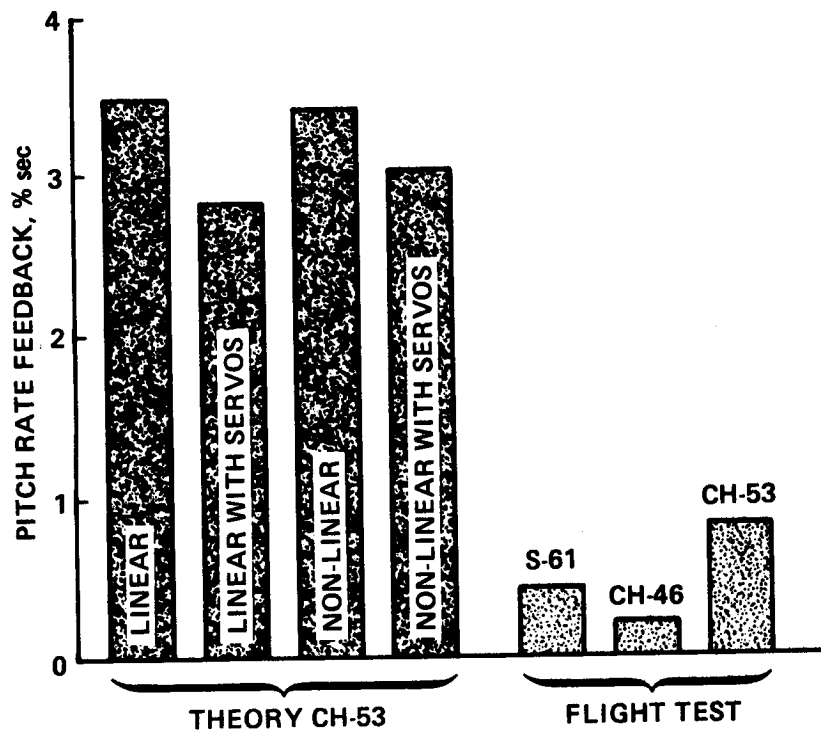
Figure 9.- Analytical and flight test gain limits for pitch rate feedback (from ref. 60).
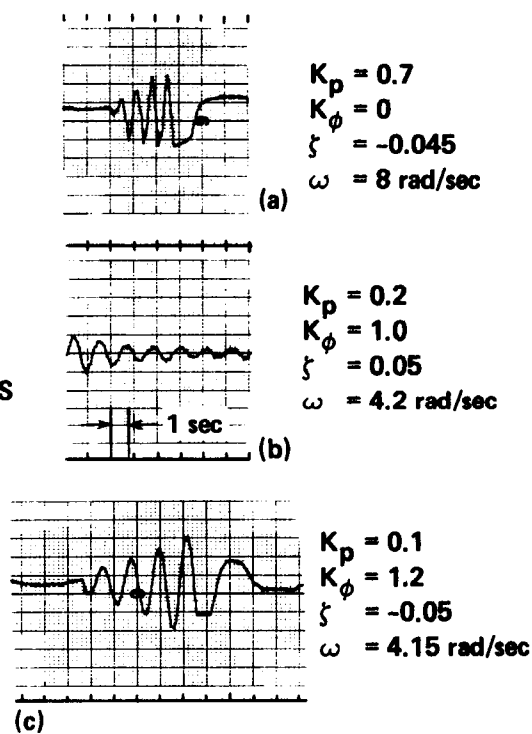
Figure 10.- Comparison of calculated and CH-47B flight test results concerning gain limits.

Figure 11.- ADOCS flight control system concept (from ref. 19).

STABILIZATION LEVEL								
	LONGITUDINAL/LATERAL				DIRECTIONAL		VERTICAL	
	RA	AT	LV	LP	RA	AT	LV	LP
AC	●				●	●	NA	
RA	●	●	●			●	NA	
AT		●	●				NA	
LA					NA		●	●
LV			●	●	NA			●

(Row header: RESPONSE COMMAND MODEL)

IDENTIFICATION CODE

		PITCH/ROLL	YAW	VERTICAL
ANGULAR ACCELERATION	AC		$\ddot{\psi}$	—
ANGULAR RATE	RA		$\dot{\psi}$	—
ANGULAR ATTITUDE	AT		ψ_H	—
LINEAR ACCELERATION	LA		—	$\ddot{h}$
LINEAR VELOCITY	LV		—	$\dot{h}$
LINEAR POSITION	LP		—	h_H

EXAMPLE: RA/AT

ANGULAR RATE COMMAND/ATTITUDE STABILIZATION

$\dot{\psi}/\psi_H$

YAW RATE COMMAND/HEADING HOLD

Figure 12.- Generic SCAS configurations (from ref. 19).

Figure 13 - Pitch axis, digital control system

δ_s → STICK FILTER

STICK SAMPLING AND SKEW

$e^{-(T/2)s}$ ω_s → θ_c^* → COMMAND RESPONSE MODEL → θ_m^* → FEED-FORWARD → $\delta_{c\theta}^*$

$\delta_{c\theta}^*$

+ e^* − δ_f^* → NOTCH FILTER → u^* → ZOH → u → ADOCS ACTUATOR → $\delta_{A\theta}$ → UPPER-BOOST ACTUATOR → $\delta_{s\theta}$ → ROTOR → δ_θ → q/δ_θ → q → $1/s$ → θ

FEEDBACK LEAD COMPENSATION ← $\delta_{f_i}^*$ + ← K_q ← q^* ← ω_s $\bar{q}$ ← ANTI-ALIAS NOISE FILTER ← SENSOR

+ ← K_θ ← θ^* ← ω_s $\bar{\theta}$ ← ANTI-ALIAS NOISE FILTER ← SENSOR

Figure 13.- Pitch axis, digital control system.

APPROXIMATE ANALYSIS METHOD

NUMERICAL PRECISION IS DECLINING

EVEN SAMPLE INSTANTS
T = 0.033 sec

$\dot{\delta}_{A_\theta}$, in./sec

TIME, sec

Figure 14.- Actuator rate ($\dot{\delta}_{A_\theta}$) response to a step input, δ_{c_θ} = 1 in.

① HOVER (BASIC)
② 70 (BASIC)
③ 130 (BASIC)
④ 130 (FULL SAS)
⑤ 130 (PARTIAL SAS)
knots

(a) PITCH/REGRESSING AND ROLL/REGRESSING MODES

(b) TIME HISTORIES OF THE 9X9 EQUATIONS (130 knots)
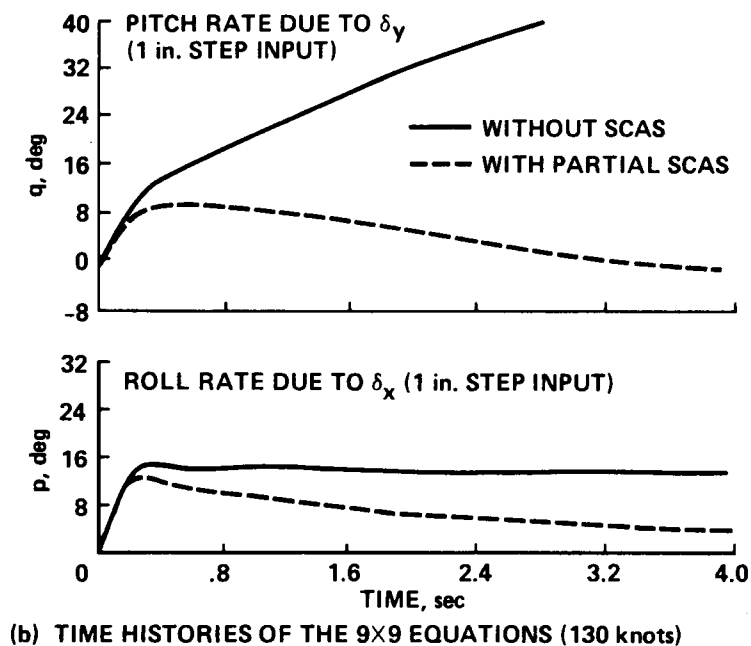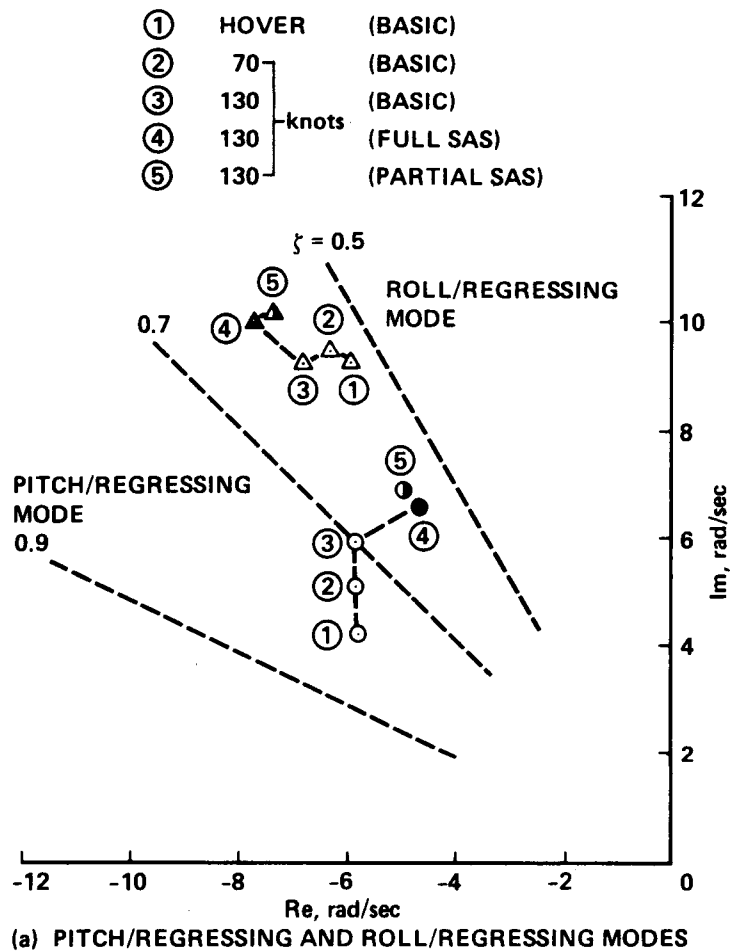
Figure 15.- Influence of flapping dynamics on SCAS performance. (a) Pitch/ regressing and roll/regressing modes. (b) Time histories generated from coupled body-flapping model.
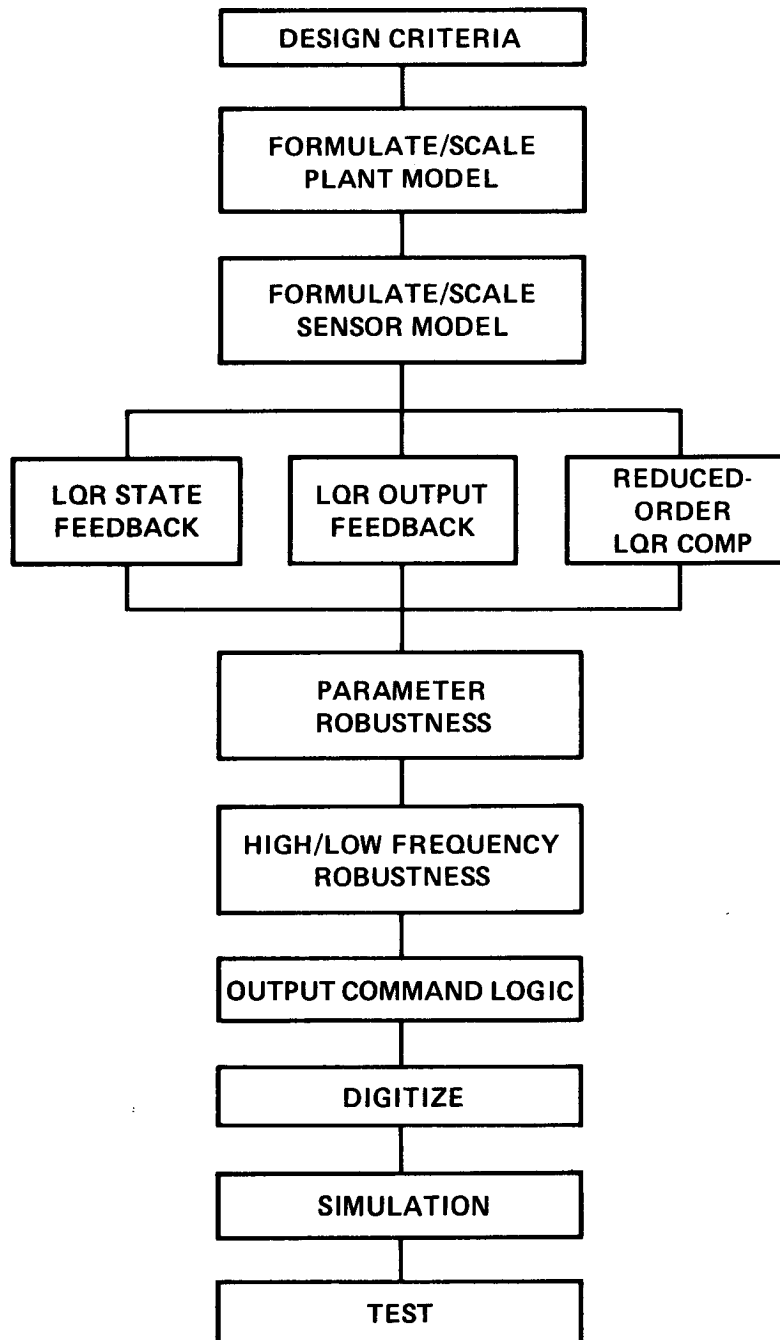
Figure 16.- The refined design methodology (from ref. 33).
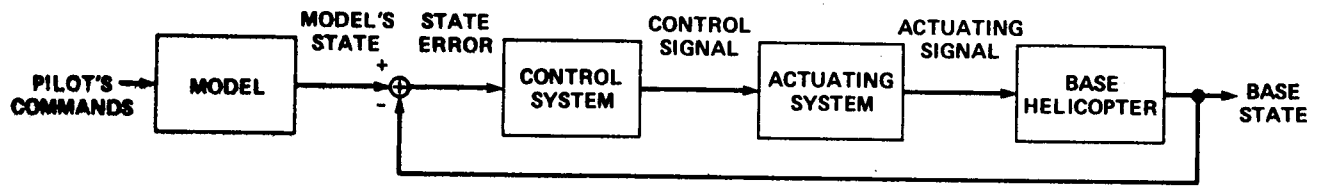
Figure 17.- Basic model-following control system concept.
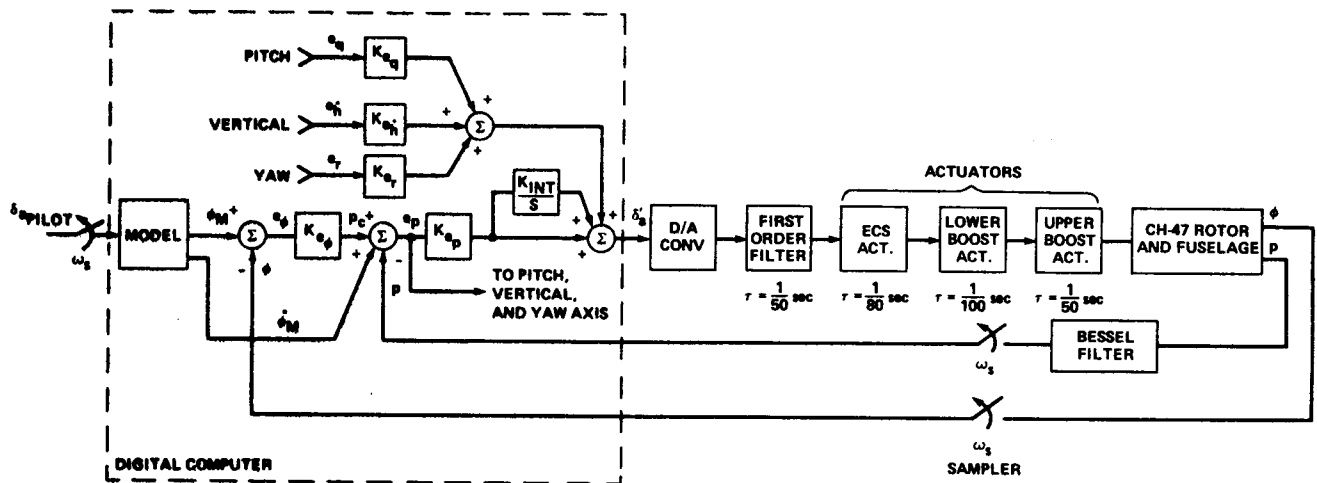
Figure 18.- Lateral model-following control system: CH-47B Implementation.
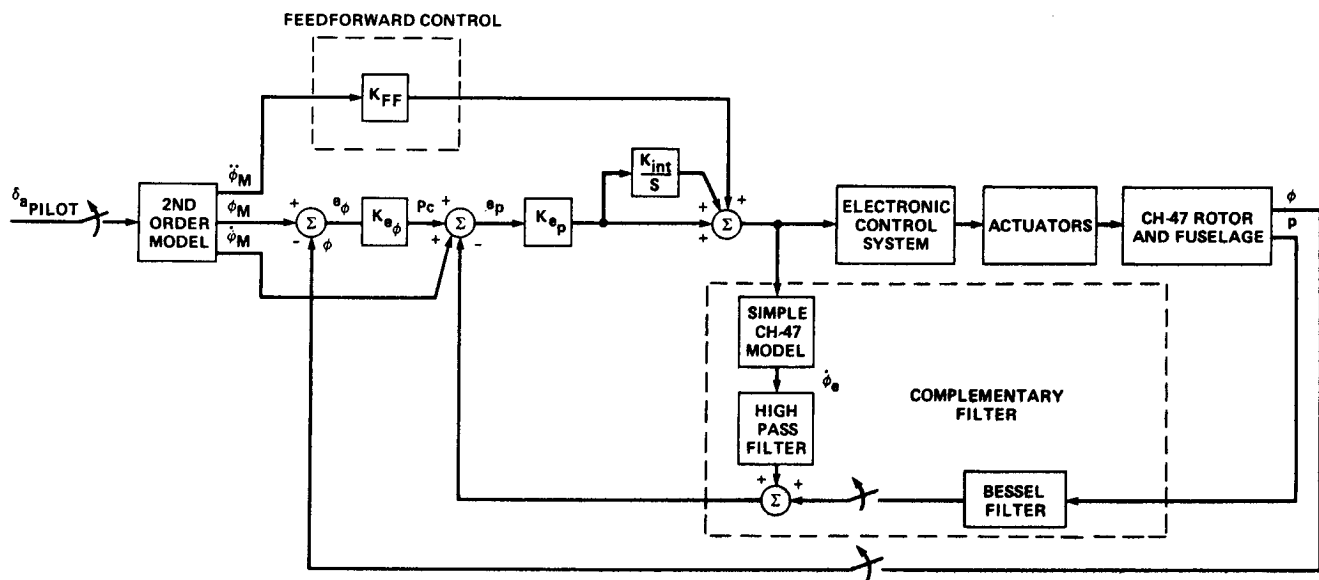
Figure 19.- Revised lateral model-following control system.
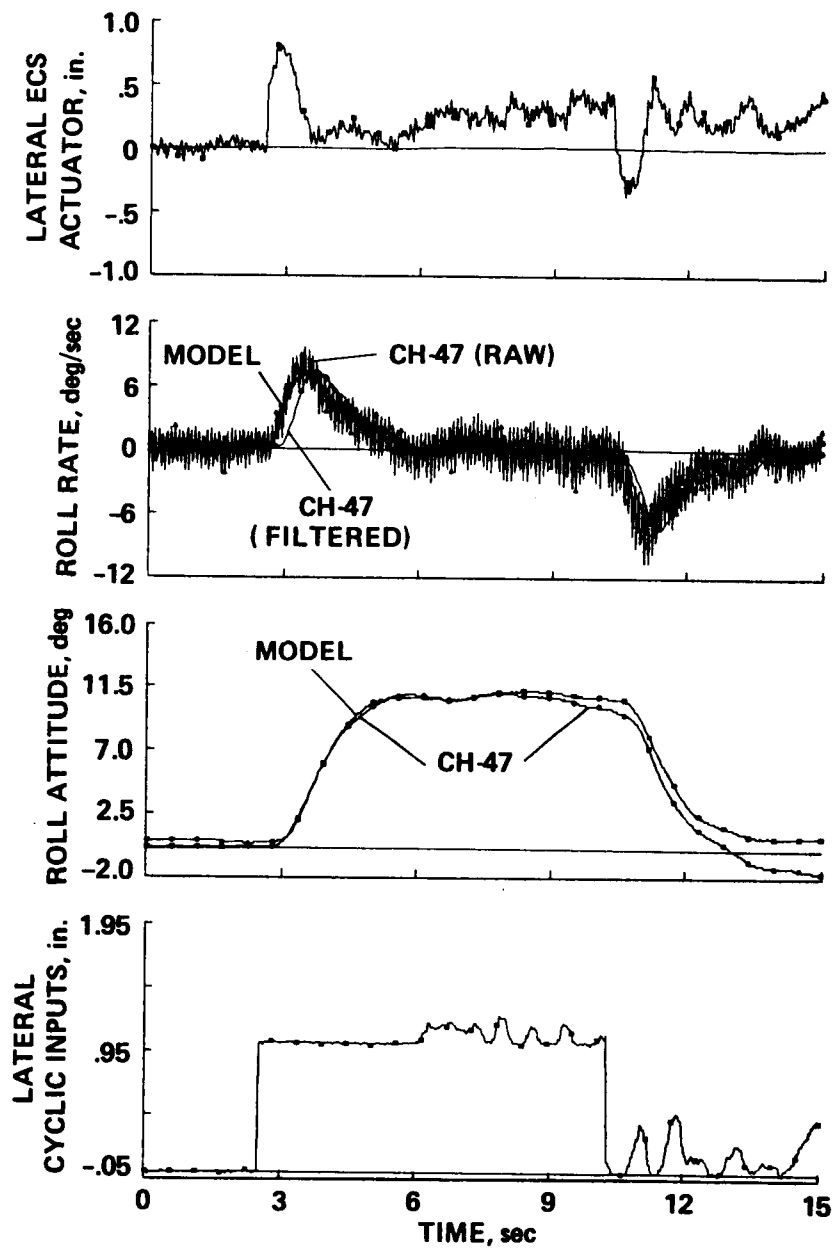
Figure 20.- CH-47B flight-test results: roll axis step response in hover.
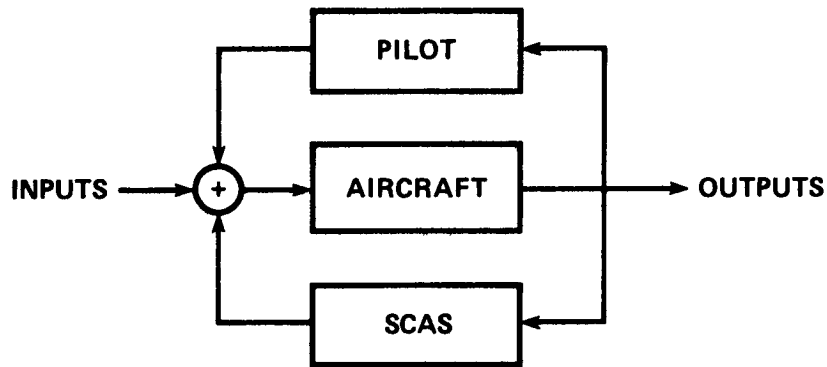
STEP 1: SET SCAS TO ZERO, SOLVE FOR OPTIMAL PILOT

STEP 2: SOLVE FOR OUTPUT FEEDBACK SCAS FOR AIRCRAFT + PILOT SYSTEM

STEP 3: SOLVE FOR OPTIMAL PILOT FOR SCAS + AIRCRAFT SYSTEM

STEP 4: REPEAT STEPS 1-3 UNTIL A STATIONARY SOLUTION IS FOUND

Figure 21.- CCS design structure.
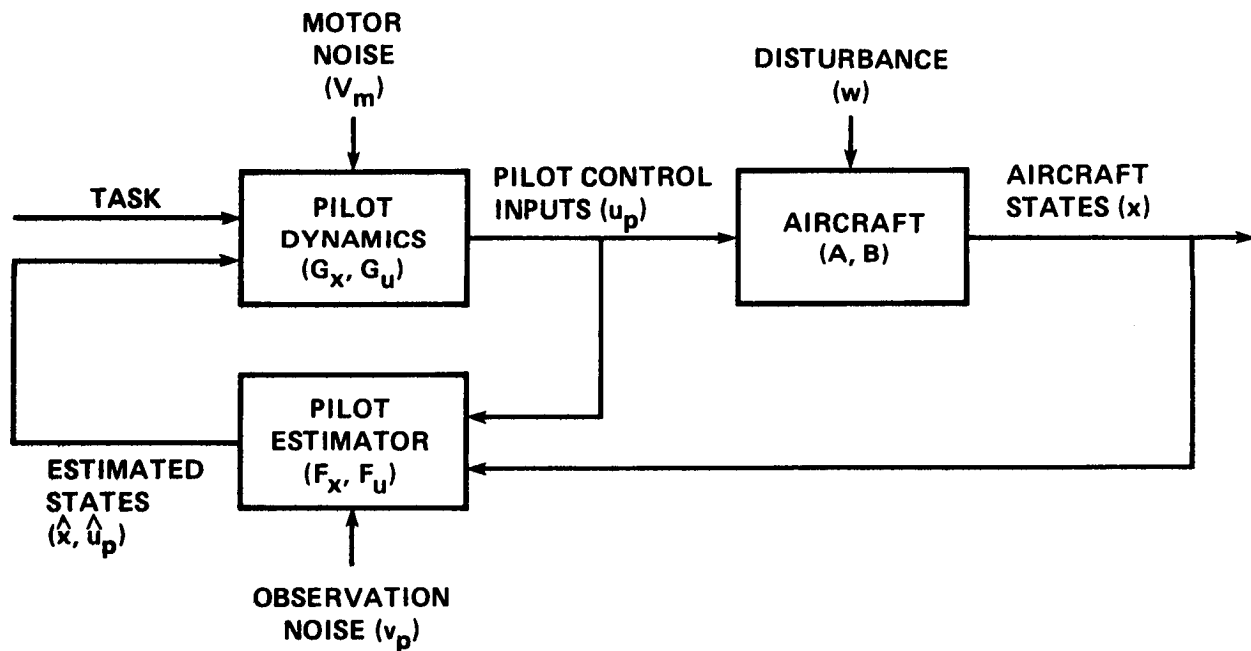
Figure 22.- Optimal pilot-model.
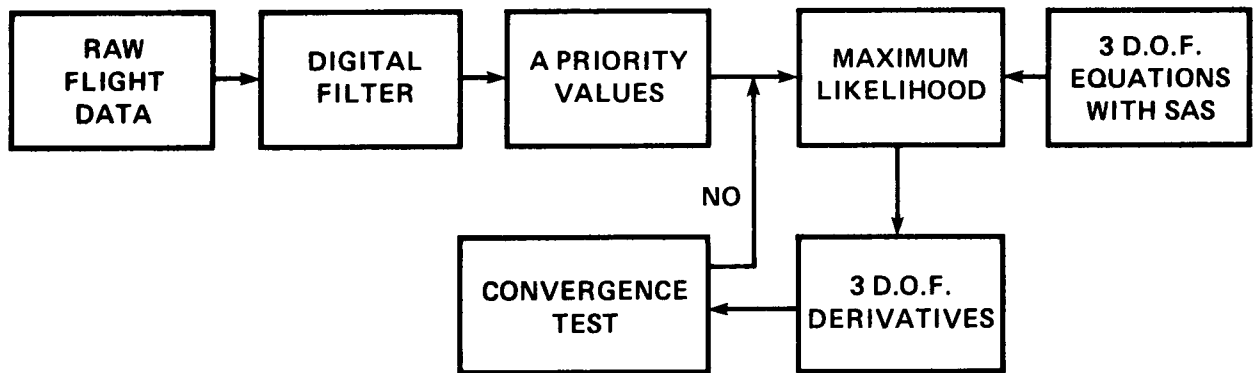
(a) MODIFIED NEWTON-RAPHSON
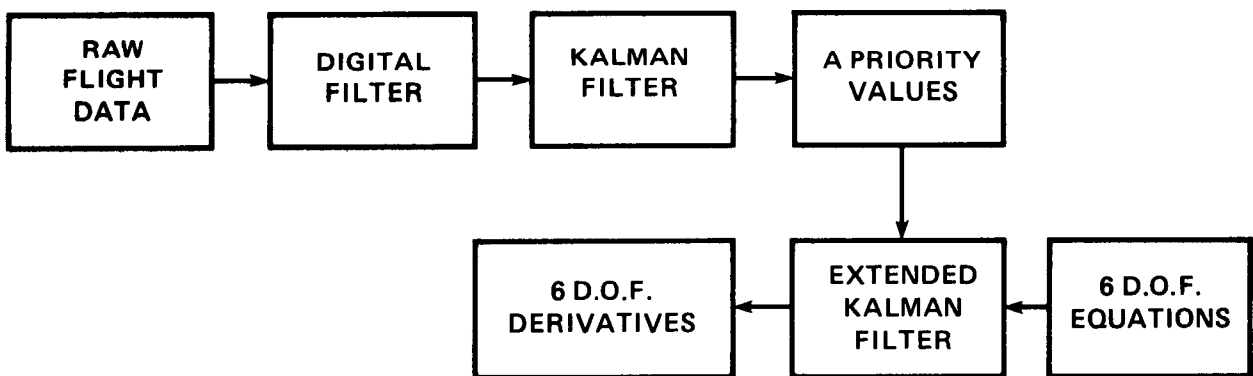
(b) EXTENDED KALMAN FILTER METHOD

Figure 23.- Parameter identification methods (from ref. 91). (a) Modified Newton-Raphson. (b) Extended Kalman filter method.
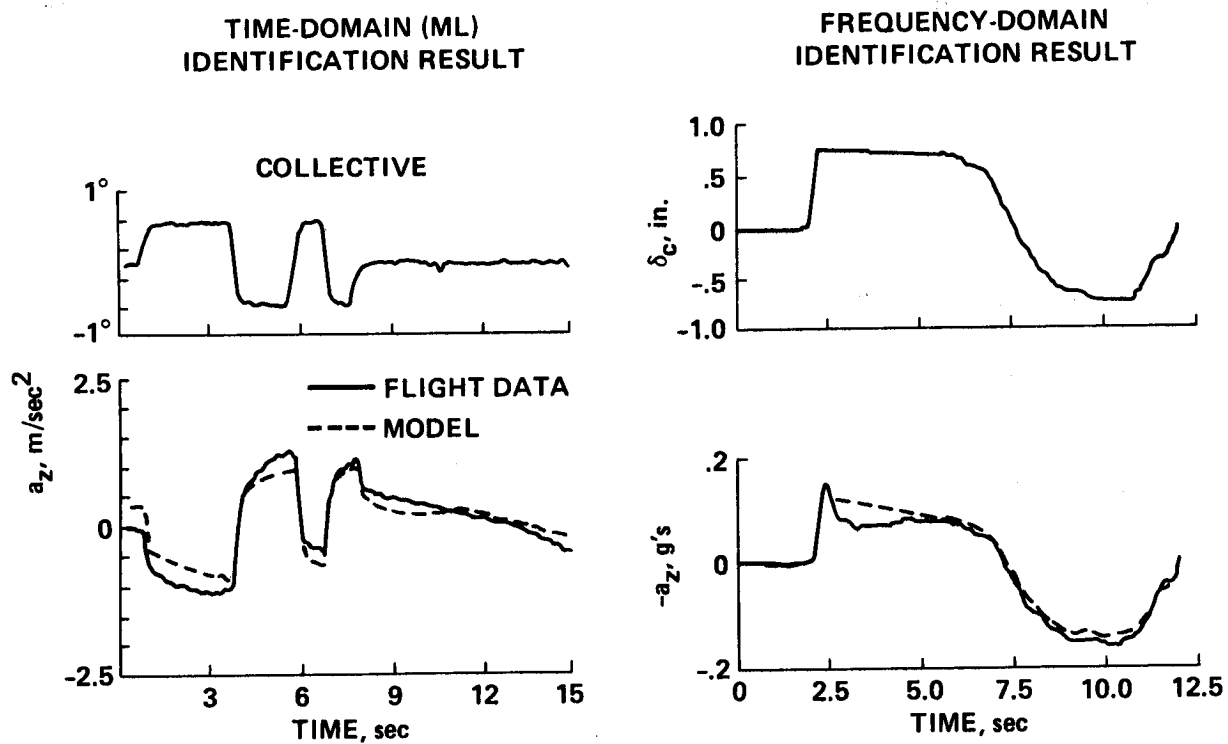
Figure 24.- Examples of time-history mismatch using good identification algorithms.
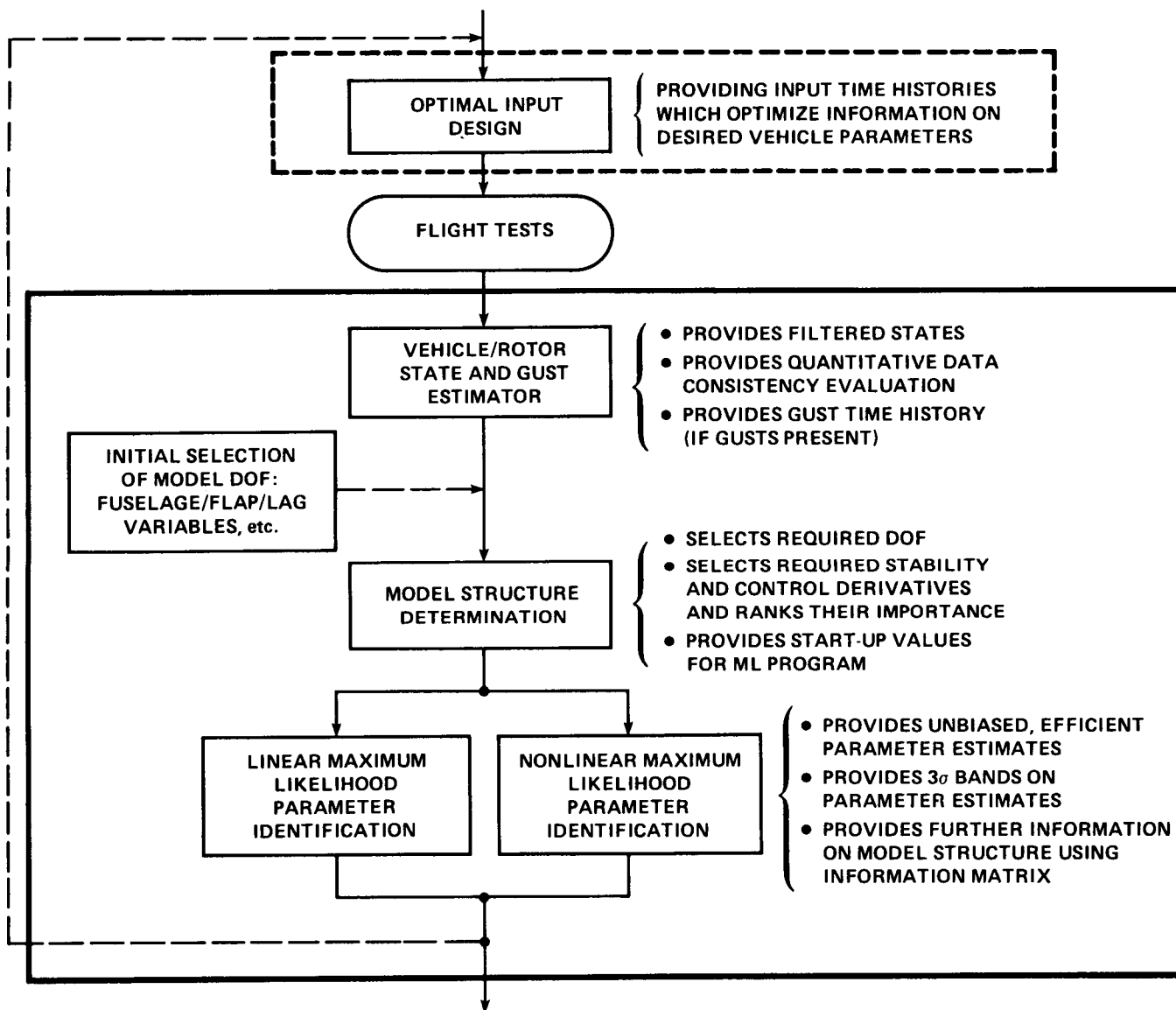
Figure 25.- Integrated rotorcraft system identification procedure (from ref. 84).
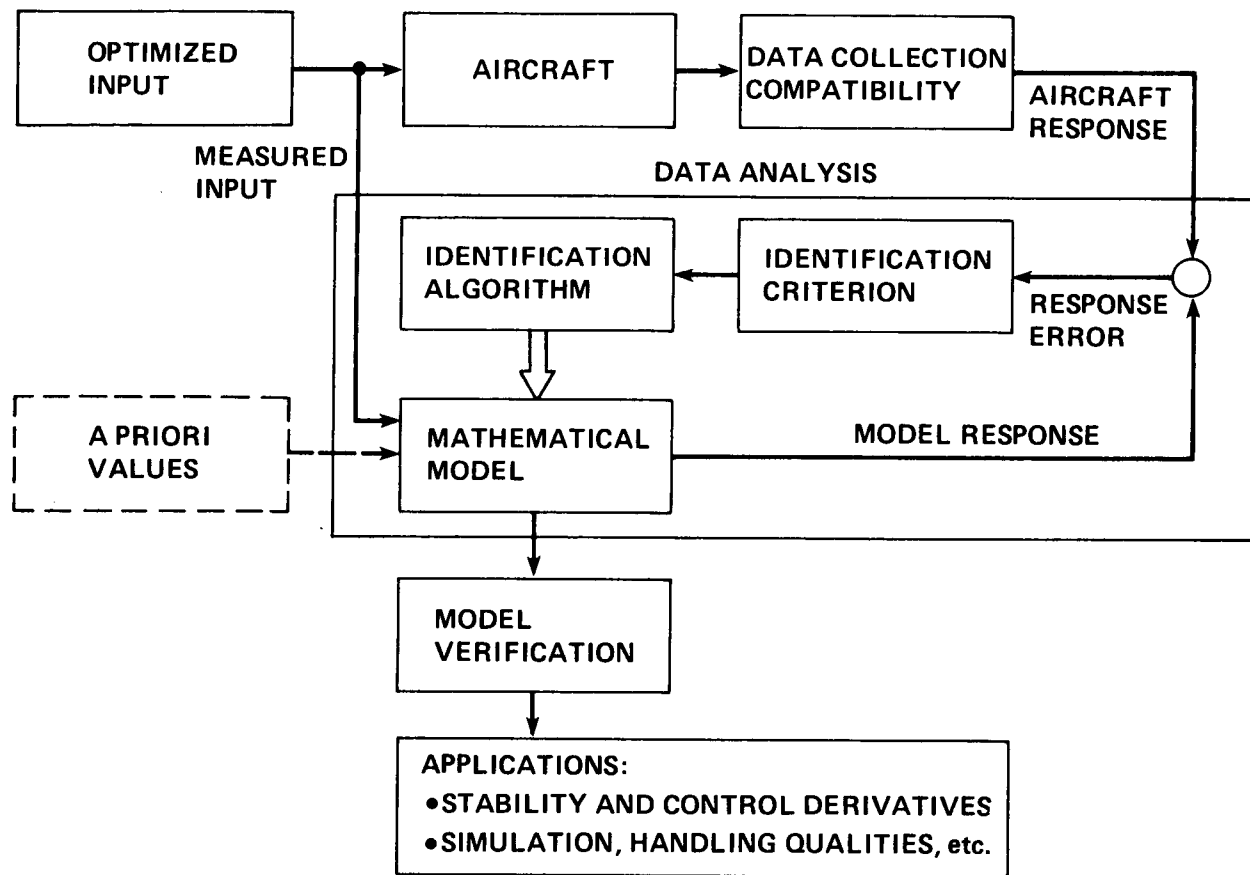
Figure 26.- Time-domain identification method.
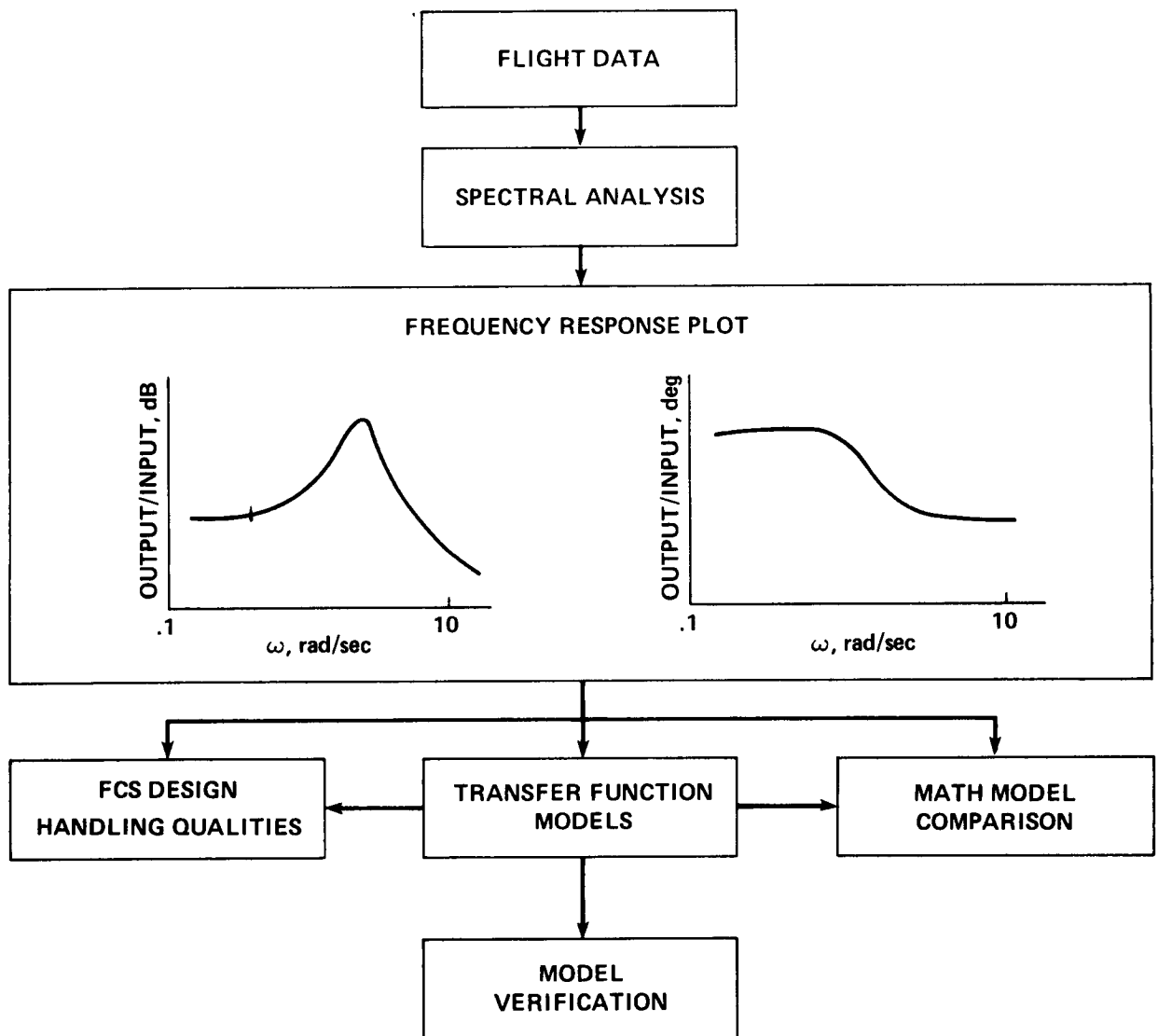
Figure 27.- Frequency-domain identification method.
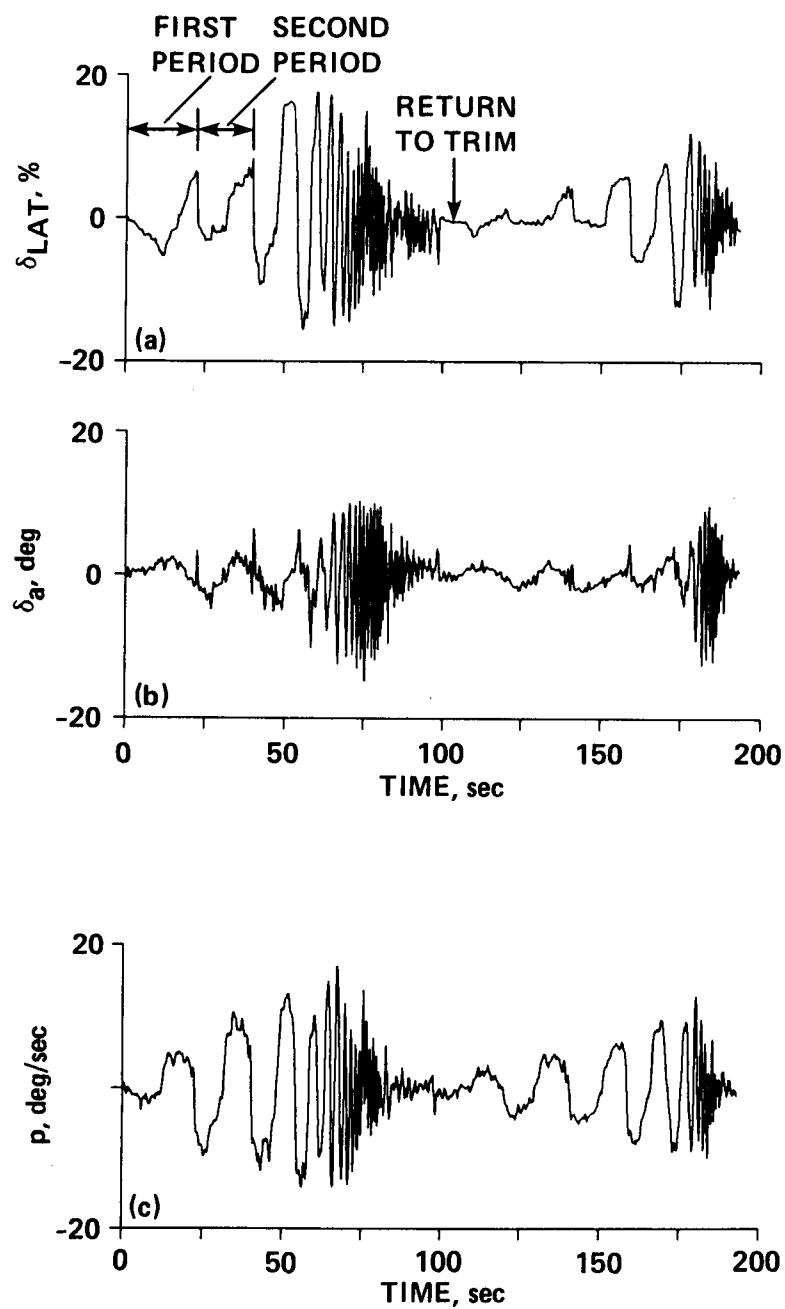
Figure 28.- Sample input and output time histories. (a) Lateral stick inputs. (b) Aileron surface deflections. (c) Roll rate response.
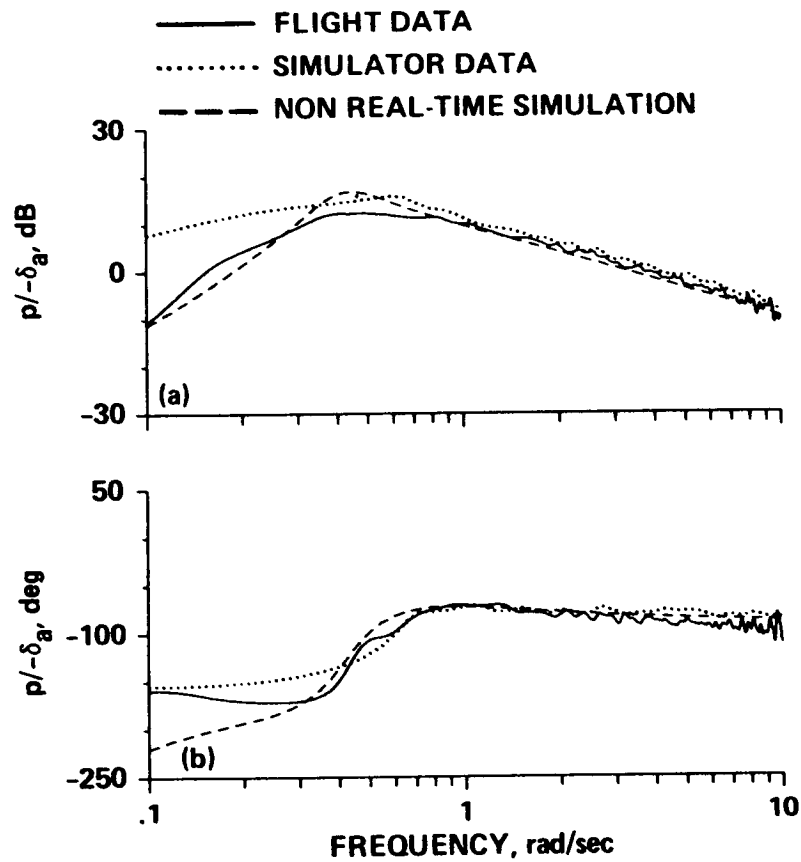
Figure 29.- Comparison of frequency response of roll rate to lateral control in hover, extracted from flight and simulation models for the XV-15.
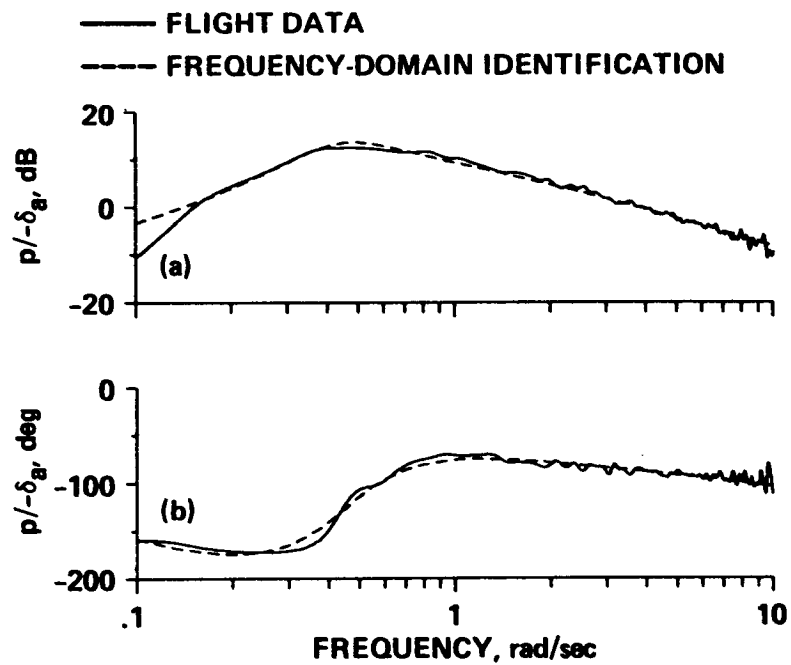
Figure 30.- Comparison of frequency responses extracted from flight with those generated from identified model.
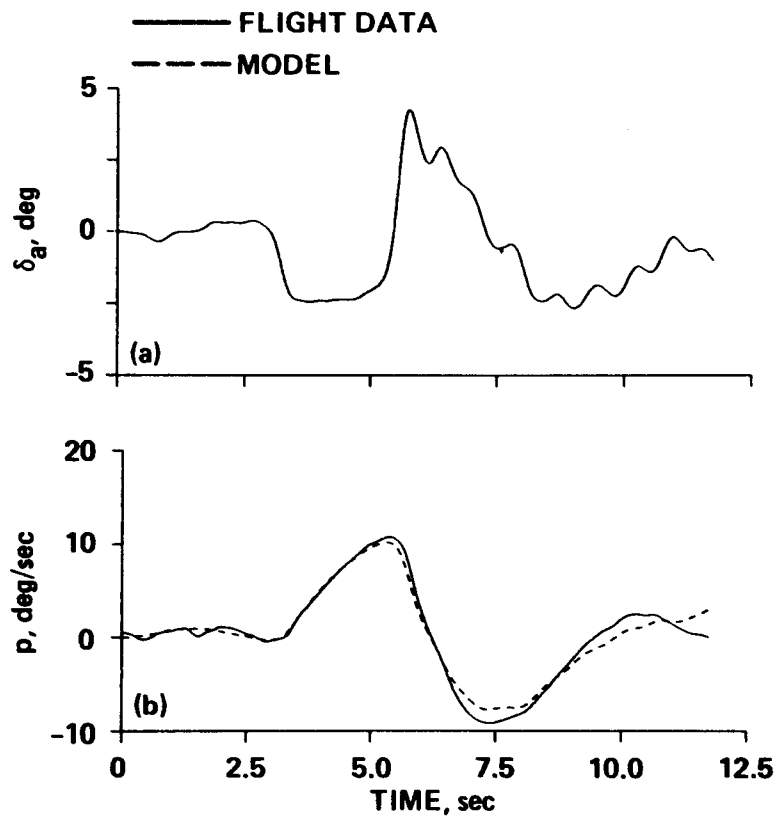
Figure 31.- Comparison of roll rate response predicted from identified model with flight data.
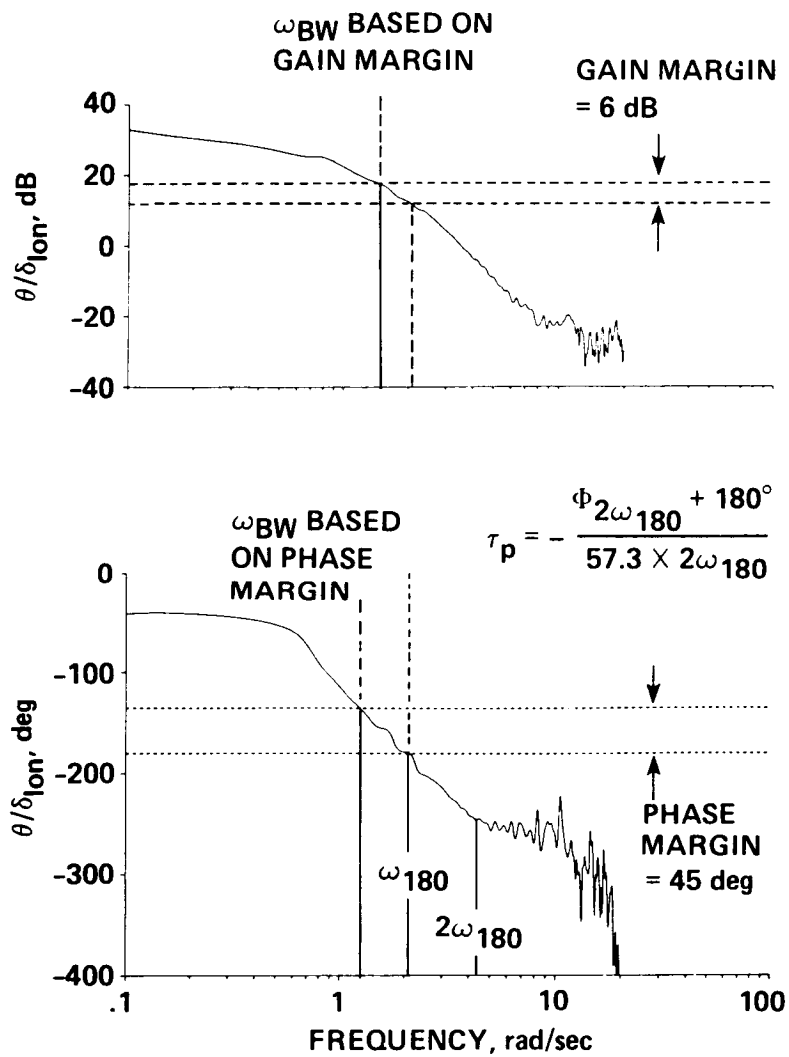

Figure 32.   Bell 214-ST helicopter.

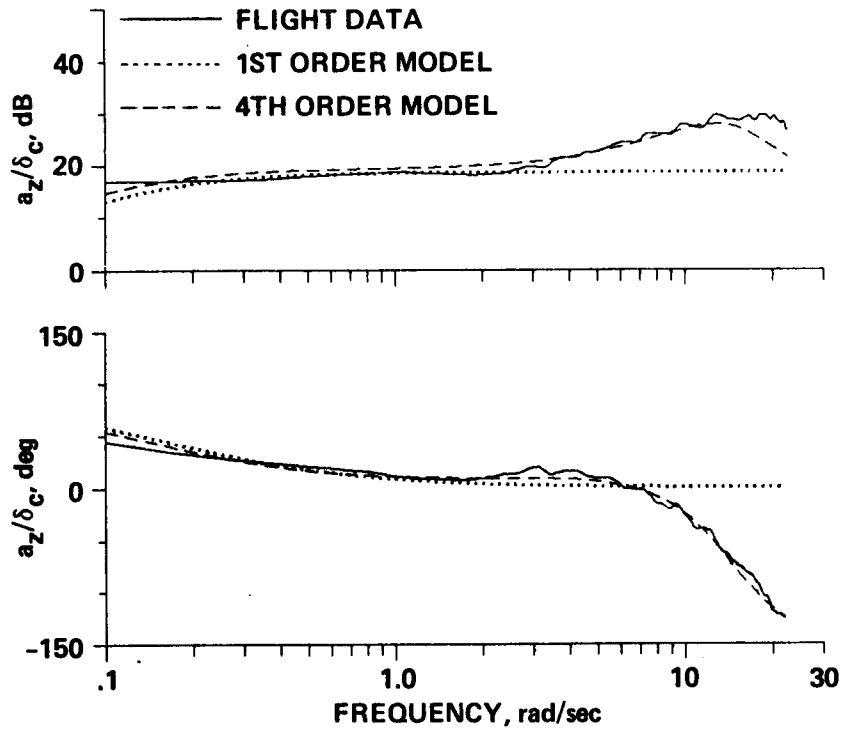Figure 33.- Identified pitch response, θ/δ_{LON}.

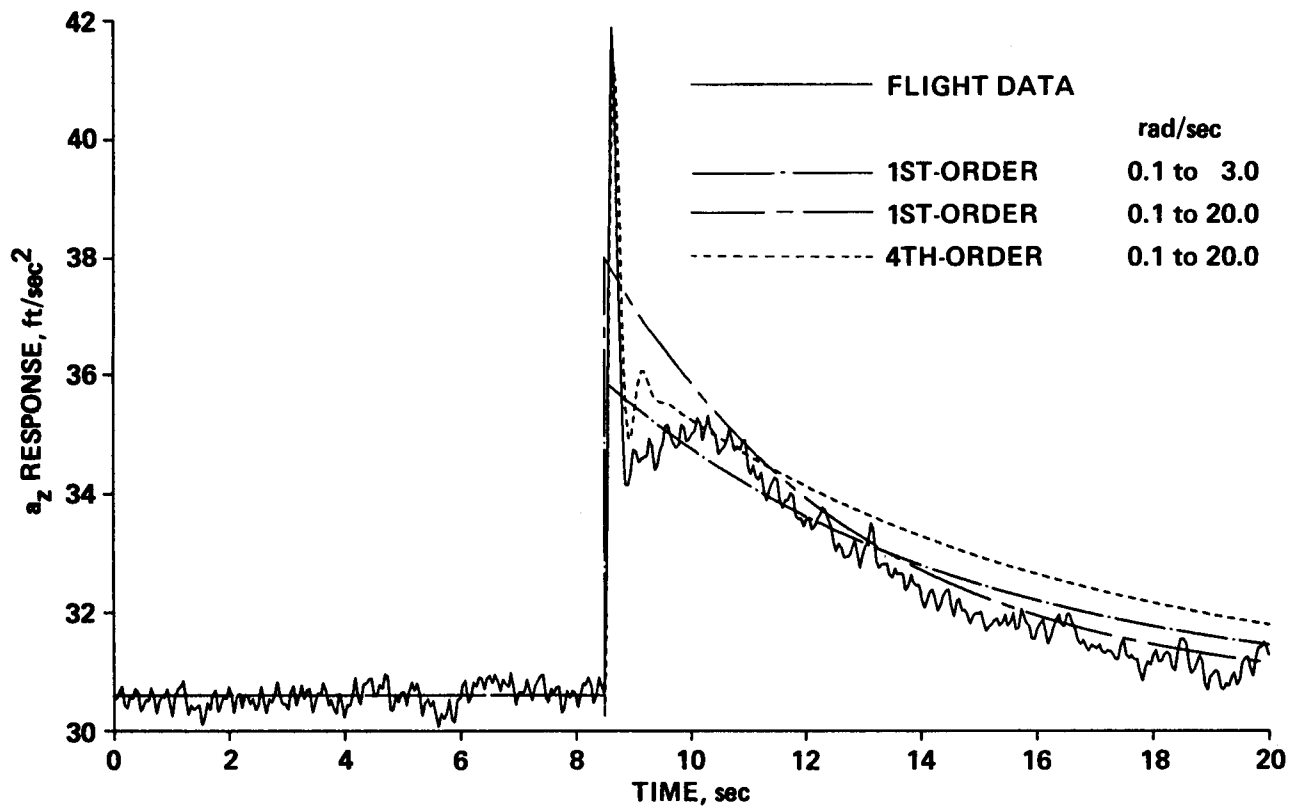Figure 34.- Transfer-function models fit to flight-extracted Bode plots of the CH-47B.

Figure 35.- Comparison of predicted responses of identified models with flight data.